1969

A study into the damage to rectangular plates subjected to dynamic loads.

Tekin, Sedat A.

Massachusetts Institute of Technology

https://hdl.handle.net/10945/13129

A STUDY INTO THE DAMAGE
TO RECTANGULAR PLATES
SUBJECTED TO DYNAMIC LOADS

by

Sedat A. TEKIN

May, 1969

COURSE XIII-A

A STUDY INTO THE DAMAGE
TO RECTANGULAR PLATES
SUBJECTED TO DYNAMIC LOADS

by

Sedat A. TEKIN

LT.JG., Turkish Navy

B.S., from Turkish Naval Academy, Istanbul, Turkey

Submitted in Partial Fulfillment of the

Requirements for the Degree of

Master of Science in Naval Architecture

and Marine Engineering

at the

MASSACHUSETTS INSTITUTE OF TECHNOLOGY

May, 1969

A STUDY INTO THE DAMAGE TO RECTANGULAR PLATES SUBJECTED TO DYNAMIC LOADS

by

Sedat A. TEKIN

ABSTRACT

Experiments are described in which rectangular mild steel plates with four edge clamped are subjected to uniformly distributed impulsive loads. The final deflections were recorded for plates with various thicknesses and subjected to different impulsive loads. It is shown that strain rate, strain hardening and finite deflections are extremely important for the large values of impact velocity.

Temperature rise on the Specimen Surfaces is investigated analytically and the Validity of some other approximations are determined.

Recommendations are made for future studies in the same general area.

Thesis Supervisor: Normal Jones

Title: Assistant Professor of Naval Architecture

ACKNOWLEDGEMENT

I wish to express my appreciation and gratitude to Professor Norman Jones, who originally stimulated my interest in the dynamic loading problems of plates and supervised this thesis. His constructive suggestions and continued encouragement were vital for the thesis.

I wish to thank Capt. D.A. Horn, Professor of "Naval Science and Naval Architecture" and Cmdr. S.C. Reed,"Assoc. Prof. of Naval Architecture" for their support in providing the Du pont detasheet explosives.

A special thanks to Dr. John W. Leech who made the "Aeroelastic Lab." available in which the experiments were carried out.

I wish to express my appreciation to Mrs. C. Hozos for typing the thesis.

Sedat A. TEKIN

TABLE OF CONTENTS

LIST OF FIGURES

Page

LIST OF TABLES

INTRODUCTION

Plastic deformation of structures under dynamic loading is quite a complex problem and due to this complexity almost no studies had been undertaken before 1940. However, recently some progress has been made on the dynamic behaviour of beams and some axial symmetric structures such as circular and annular plates.

As far as the author is aware, no study has been done up to present, on the dynamic behaviour of rectangular plates.

Therefore, the main object of the thesis is to investigate the behaviour of a rectangular plate, which is a common engineering structure, when subjected to impulsive loading in order to provide valuable data necessary for future theoretical studies.

The dynamic plastic behaviour of structures is clearly a function of several variables. However, reasonable approximations, such as ignoring the influence of strain hardening and elasticity of the material, may provide accurate prediction of the behaviour of a structure when loaded dynamically. A rigid-perfectly plastic material is shown in figure (1). This idealization, in plasticity theory, yields great simplifications for various engineering problems.

In fact, analytical and theoretical studies show that strain hardening is unimportant up to the order of twice the plate thickness Ref.(1).

Definations of the lower and the upper bound theorems for rigid-perfectly plastic materials are given in many references. For example Ref.(2):

Lower bound theorem: "...... If a system of stresses can be found

which is in equilibrium with the applied loads and which nowhere violates yield, then the structure will not collapse". Ref.(2)

Upper bound theorem: "...... If the work of a system of applied loads due to an associated kinematically admissible displacement field is equated to the corresponding internal work, then the system of loads will cause collapse of a structure". Ref.(2)

It is obvious that from the definition of the upper and the lower bound theorems, the upper bound theorem always gives greater values of the applied loads than the lower bound theorem. When these two theorems yield the same result, then the solution is an exact one. In this case, the results would give the greatest load which the structure may withstand without failure. A complete discussion of the dynamic behaviour of beams has been considered by LEE and SYMONDS Ref.(3). However, in the case of two dimensional structures the problem is more complicated. Some solutions for axial symmetric structures such as circular and annular plates has been obtained. Ref.(4,5,6)

HOPKINS, PRAGER and others have considered the limit analysis of plates for bending only.

Simultaneous influence of membrane forces and the bending moments has been given by JONES. Ref.(7) His theoretical study on a simply supported rigid-perfectly plastic annular plates shows that final deformations are considerable smaller than those obtained by a bending theory only. Ref.(8) A theoretical study on the behaviour of a simply supported rigid-perfectly plastic circular plate has been given by the same author. Ref.(9) His valuable results indicate that the

plate could support greater pressures when finite deflections are taken into account.

COX and MORLAND have determined the load carrying capacity of a simply supported square plate. Ref. (10). They neglected elasticity, work hardening and strain rate effects and they estimated error due to approximation of Tresca's yield criterion to Johansen's criterion would be about five per cent.

However, it does not appear possible to extend these solutions in order to describe the behaviour of rectangular plates. As a matter of fact, there is no exact solution, at present, for rectangular plates even when loaded statically. Difficulties arise due to anti-symmetric velocity field and the appearance of twisting moments in the equilibrium equations. Hinge line patterns of rectangular plates are shown in figure(2). When the upper bound collapse mechanism is used to describe the behaviour of a rectangular plate, it is assumed that all the deformations are confined to the hinge lines while the rest of the plate including the boundaries remain rigid.

It is clear from the foregoing comments that it would be extremely difficult to obtain a theoretical solution which describes the dynamic behaviour of a rectangular plate. The analysis would become even more complex if the influence of finite deflections were retained in the basic equation as they should be for circular plates with axial restraints. It is clear, therefore, approximate but reliable methods should be developed in order to describe the behaviour of rectangular plates as well as more general structural shapes when subjected to dynamic loads.

It is hoped that the experimental results presented here will aid in the development of these approximate theories as well as providing useful design information.

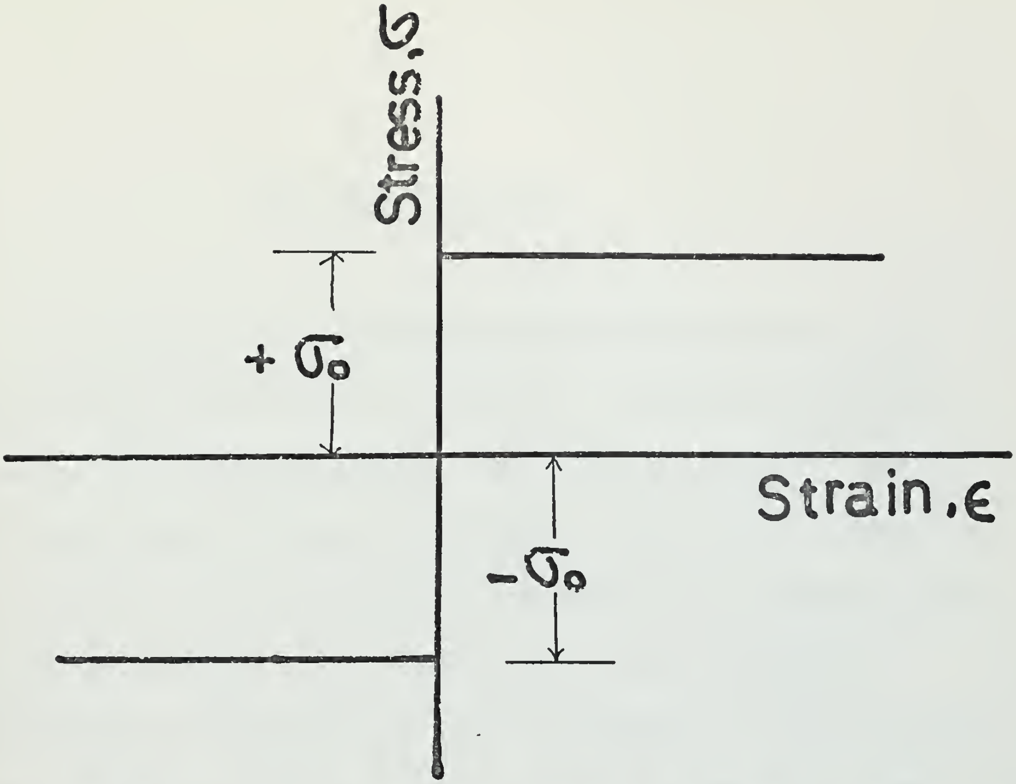

Fig.1 Rigid perfectly plastic material

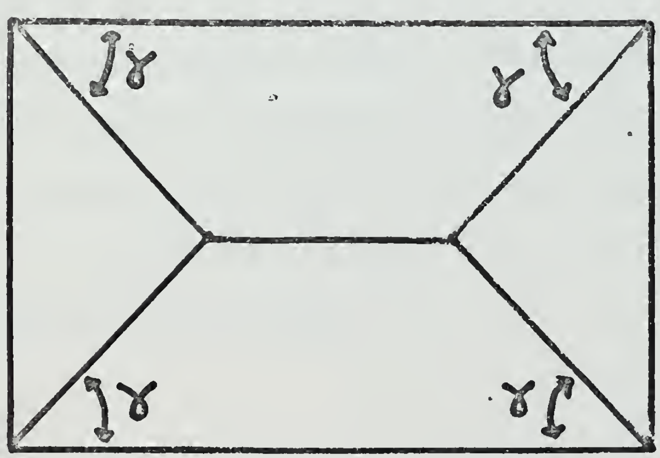

Fig.2 Hinge line patterns of a rectangular plate

BALLISTIC PENDULUM

One of the basic values which must be calculated is the external energy applied to the structure. The applied impulsive load can be determined in several ways depending upon the nature of the load. There are many satisfactory experimental techniques in the field of dynamic loading of structures. One example is the "Impact Tube Technique", which has been developed recently. Essentially it is an adoptation of the aerodynamic shock tube which is used for appling impulsive loads to plates of various geometrical shapes. A more detailed description of the impact tube has been given in Ref.(11). However, the simplicity and the economical considerations compel the use of a ballistic pendulum.

It is apparent that notwithstanding the disadvantageous which are listed in the recommendation section of the thesis, the ballistic pendulum is a quite satisfactory technique which can be used to study the impulsive loading of structures.

The impulse imparted by an explosive lying on the specimen surface, can be computed by the initial amplitude of the ballistic pendulum swing as in the following manner.

From conservation of momentum,

$$I\omega_0 = mR(V_0 - R\omega_0) \qquad (1)$$

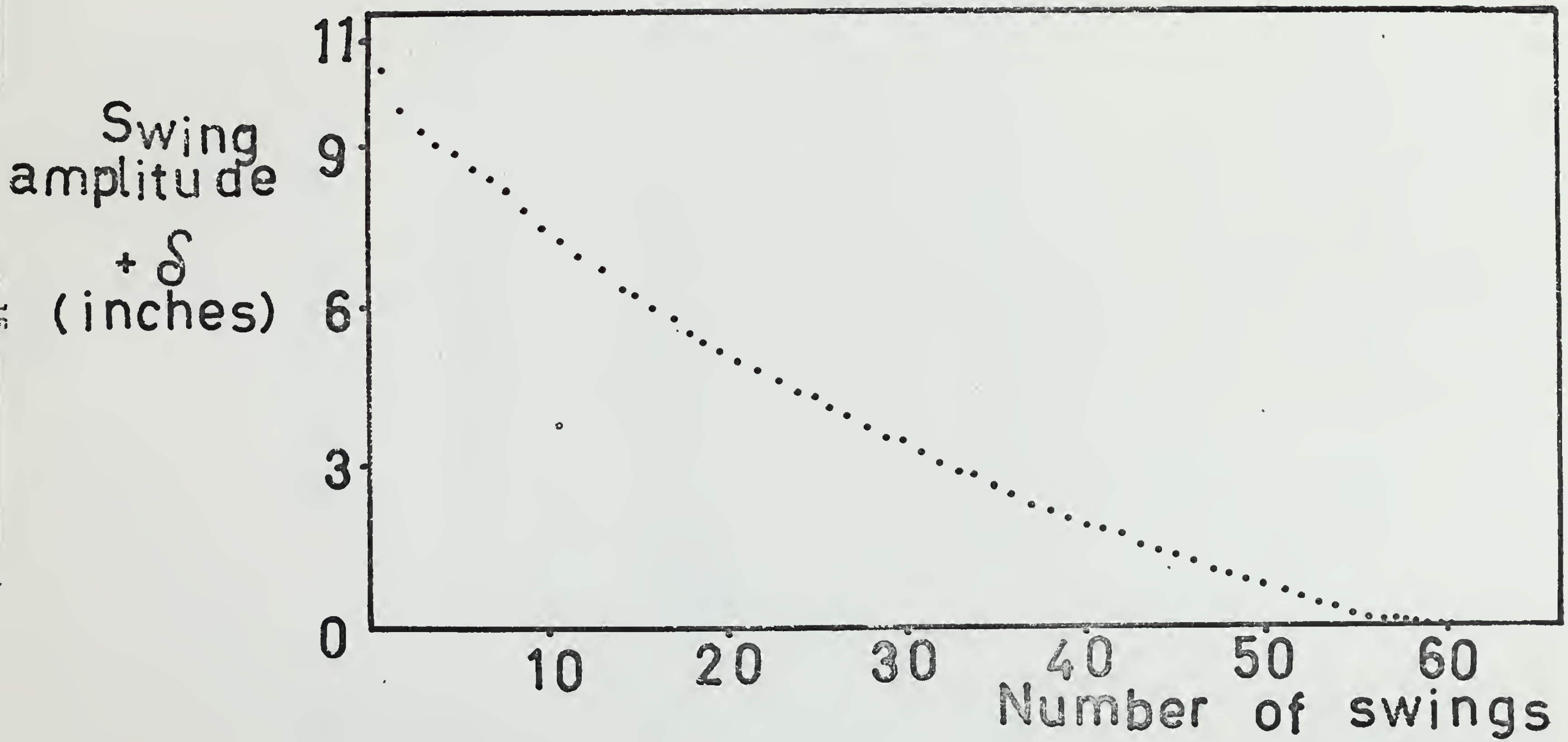
Swing
amplitude
+ δ
(inches)
11
9
6
3
0
10
20
30
40
50
60
Number of swings

Fig. 3

Neglecting, friction losses at pivots, air drag forces and the energy dissipation due to unballanced swing conservation of energy can be written; Ref.(12)

$$\frac{1}{2}(I+i)\omega_o^2 = g(m+M)R^*(1-\cos\theta_m) \tag{2-a}$$

or,

$$\frac{1}{2}(I+i)\omega_o^2 = 2g(m+M)R^*\sin^2(\tfrac{1}{2}\theta_m) \tag{2-b}$$

Combining Equ.(1) and (2)

Impact velocity, $V_o = \dfrac{\sqrt{2g(I+i)R^*(1-\cos\theta_m)(m+M)}}{mR}$ (3)

when $m \ll M$ and $R \cong R^*$, Equ.(3) can be written:

$$V_o = \left(\frac{2}{m}\right)\left(\sin\frac{\theta_m}{2}\right)\sqrt{\frac{gIM}{R}} \tag{4}$$

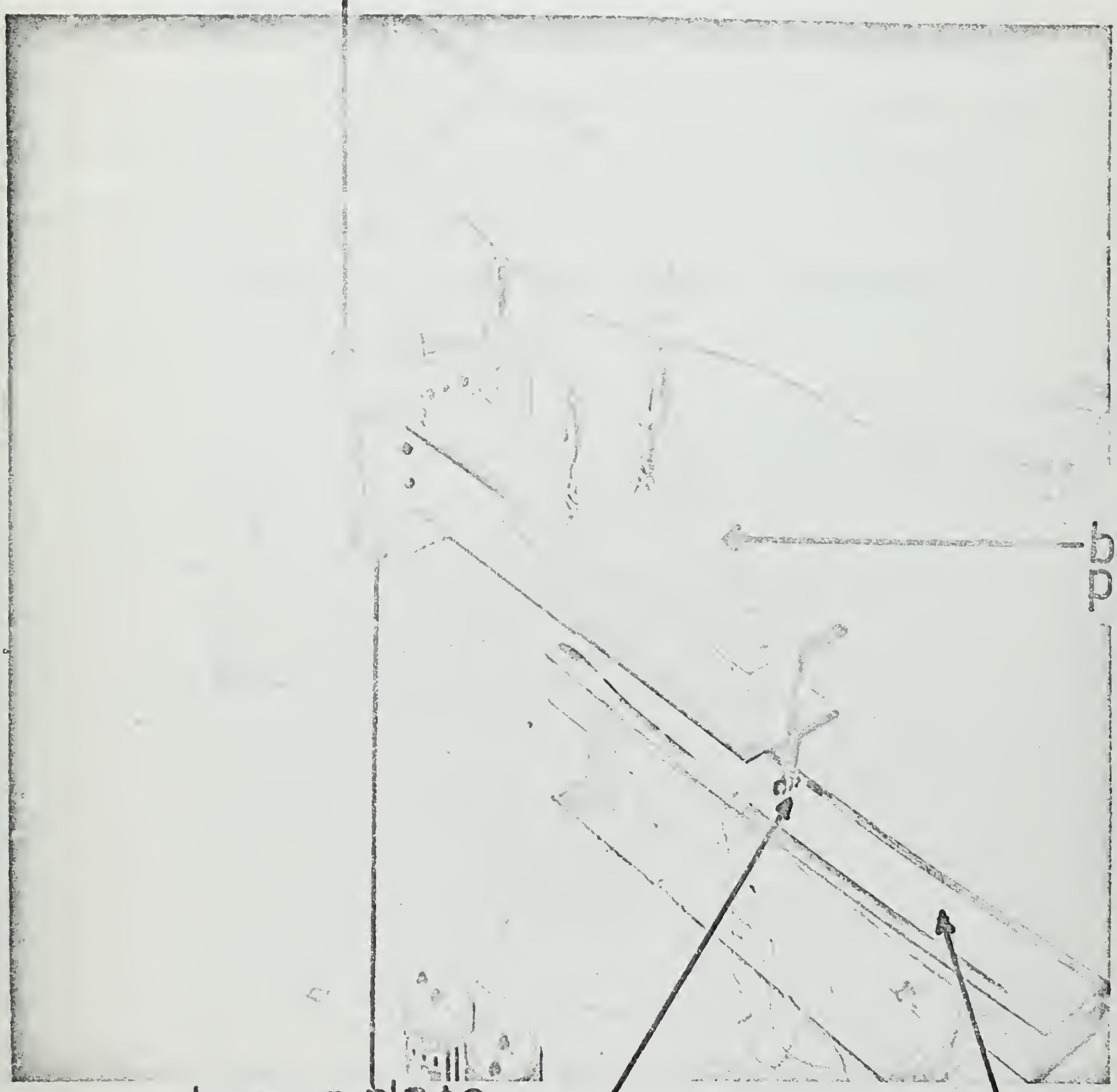
upper head
ballistic
pendulum
lower plate
hotwire
heat sensitive
paper

Fig. 4

The validity of the above approximations i.e. $m \ll M$ and $R \cong R^*$ are given in Appendix C.

It may be seen from the results presented in Appendix C that the difference in impact velocity, V_o calculated from Equ.(3), and (4) is 0.15% approximately for Vo 250 ft/sec. and about 0.147% for Vo 100 ft/sec. It is also shown from Fig.(3) that energy losses due to air drag and friction forces at pivots are negligible and, therefore, they may not be taken into account.

In the following two pages, impact velocity calculation of the specimen No=190 is presented.

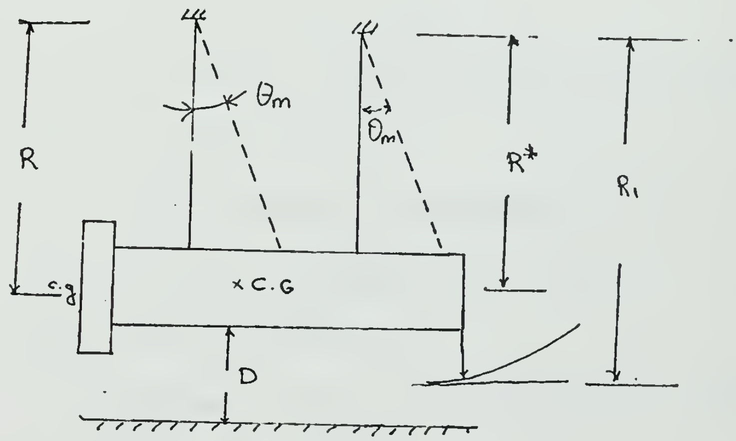

Fig.10

Impact Velocity Calculation of Specimen No=190:

$$\text{Impact velocity, } V_o = \frac{\sqrt{2g\,(I+i)\,R^*\,(1-\cos\theta_m)\,(m+M)}}{mR}$$

Specimen weight, $m = \rho \times S \times H = 1.94274 \times H$ kg.

ρ = density of mild steel, kg/in.^{3}

S = surface area of the specimen =15.1875 sq.in. (constant for all experiments)

H = thickness of the specimen

In this example, H = .17251 in. (Table 2 or 3)

Total weight of pendulum = (m + M) kg.

In this example (m + M) = 40.4795 kg. (Table 2)

R = distance from pivots to c.g. of the specimen, see Fig.(10)

R = 138.8 - D - (2.5) = 136.3 - D in.

D = distance from ground (Table 2)

In this example, D = 7.75 in.

Therefore, R = 136.3 - 7.75 = 128.55 in.

$R - R^*$ = shifting of the c.g. due to ballast loads.

$$R - R^* = \frac{\text{ballast loads} \times 2.5}{(m + M)} \text{ in.}$$

ballast loads = (m + M) - $(\text{constant})_{1,2,3}$

$(\text{constant})_1$ = 32.6545625 (for thin specimens)

$(\text{constant})_2$ = 32.8645 (for medium specimens)

$(\text{constant})_3$ = 33.6795 (for thick specimens)

In this example, $R - R^* = \frac{2.5\ [(m+M) - 33.6795]}{(m+M)} = 0.4199$ in.

Therefore, $R^* = R - 0.4199 = 128.55 - 0.4199 = 128.13$ in.

$$I = (m+M)R^* = (40.4795) \times (128.13)^2 = 6.64563 \times 10^5 \text{ kg-in.}^2$$

$$i = (0.194125 \times 0.17251)\ (128.55)^2 = 554.9728 \text{ kg-in.}^2$$

$$(I+i) = 665118.9427 \text{ kg-in.}^2$$

Maximum swing angle, $\Theta m = \frac{7.75}{133.55} = 0.05833$ Radians

$$= 3^{\circ}.34$$

Substituting the values of $(I+i)$, $\cos\Theta m$, R^*, $(m+M)$, m and R into Equ.3

$V_o = 128.59479$ ft. per sec.

Computer result: $V_o = 130.707$ ft. per sec.

(1.6165% error due to approximate cosine value of $3^{\circ}.35$ given in the Mathematical Tables).

EXPERIMENTAL DETAILS AND DESCRIPTION

The experiments were performed in the "Aeroelastic and Structures Research Lab." at Massachusetts Institute of Technology.

In all the experiments Du pont blasting capsules - No = 6 and Du pont Detasheet - D explosives were used. The average size of the detasheet leader used to connect the detonator to the exploxive sheet was 1/8 in. thick and 12-20 in. long. The dynamic behaviour of the rectangular plates was studied with the aid of the ballistic pendulum shown in Fig.(4). The maximum deflections of the ballistic pendulum were measured by a hot wire passing over heat sensitive paper which was placed on a device having the same curvature as the swing path of the pendulum.

Rectangular plate specimen 8 in. by 6 in. were drilled with 3/8 in. diameters, 95 shown in Fig.(5). High strength steel bolts and nuts were used to clamp the specimens securely between the lower and upper heads as shown in Fig.(6). The specimens used in the first group of experiments were only machine grinded while polishing was done manually with "fine emery cloth". The rest of the specimens (Sp. No = 60, 70, 80, 90, 100, 180, and 190) were machine grinded and polished.

Prior to detonating the explosive, the flatness of each specimen was inspected and the thickness measured. For each plate 32 thickness readings were measured and the average of these was taken as the actual thickness of the plate. Deformations were measured with the

aid of a surface plate and a dial gage having an accuracy of 0.0001 in. The required boundary conditions was achieved by clamping the specimen securely between the lower and the upper head. In order to prevent any slip of the specimen, grooves were machined on the facing sides of the head as indicated in Fig.(7).

Two types of shock absorbers, namely neoprene and foam rubber were used in the experiments to prevent the "spalling effect" caused by a sharp fronted stress wave with an amplitude greater than "critical fracture stress" of the material. In addition to foam rubber two layers of drafting tape - No=230 was mounted between detasheet explosive and the specimen surface in order to prevent the "pitting effect" of the high explosive temperature. (In Table II, the notations N and F refer to neoprene and the foam rubber respectively). The weights and the dimensions of the neoprene, foam rubber and the drafting tape are given in the following table.

	Thickness	Surface area	Weight
Neoprene:	0.1242 in.	$3x5\frac{1}{16}$ sq.in.	42 grm.
Foam rubber:	0.4968 in.	$3x5\frac{1}{16}$ sq.in.	7 grm.
Drafting tape:	$5x10^{-3}$ in.	$3x5\frac{1}{16}$ sq.in.	--
Rubbery cement*:	--	$3x5\frac{1}{16}$ sq.in.	--

(Table I)**

The locations of the foam rubber (or neoprene) and the detasheet

* It was used to glue the foam rubber (or neoprene) and the detasheet explosive.

** The physical properties of foam rubber and neoprene are presented in Appendix D.

explosive on the specimen surface are shown in Fig.(8). In all calculations the weight of the foam rubber and neoprene were neglected. (See Appendix C). Commercially, the thinnest detasheet explosives are produced with two standard thicknesses of 10 mils and 15 mils. In order to study in a wide range of the impulsive loading, some holes were punched on some of the detasheet explosives, as indicated in Fig.(9), and it was assumed that the loading characteristics of the impulse would remain unchanged.

Impact velocity calculations were performed by an IBM/1130 and the rest of the calculations were done on a Wang calculator.

Careful attention should be paid to ballancing of the ballistic pendulum otherwise vibration may cause undesirable energy dissipation. In order to achieve perfect ballance of the ballistic pendulum lead blocks with different weights were used and their effects were considered in the calculations.

The apparatus used in this experimental study were prepared by R. Van Duzer, LT. U.S.N.; R. Griffen, LT. U.S.N.; T. Uran, LT.JG., T.N. and by the author.

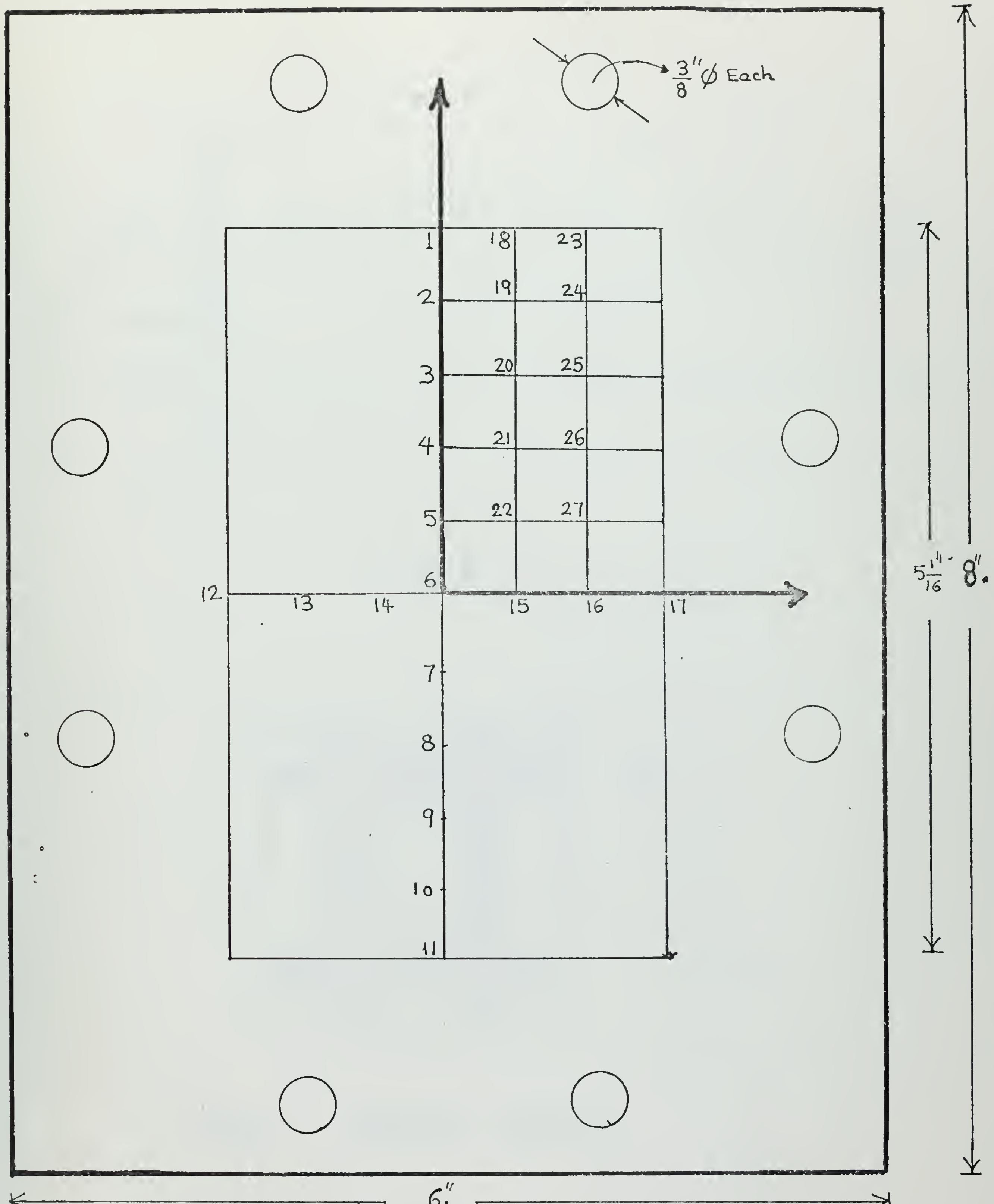

Fig.5 The location of the X-Y coordinate axes on a full scale specimen
(POINT NOS. INDICATE WHERE THE DEFORMATIONS ARE MEASURED.)

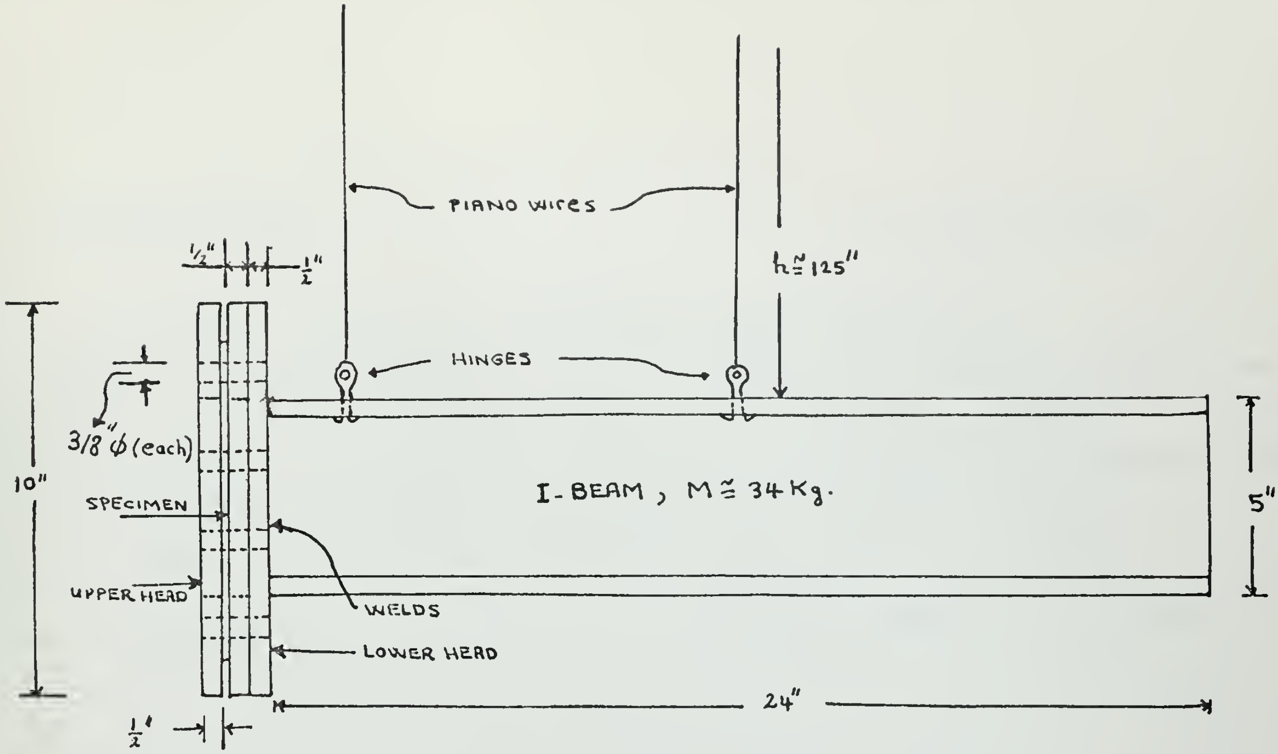

Fig.6

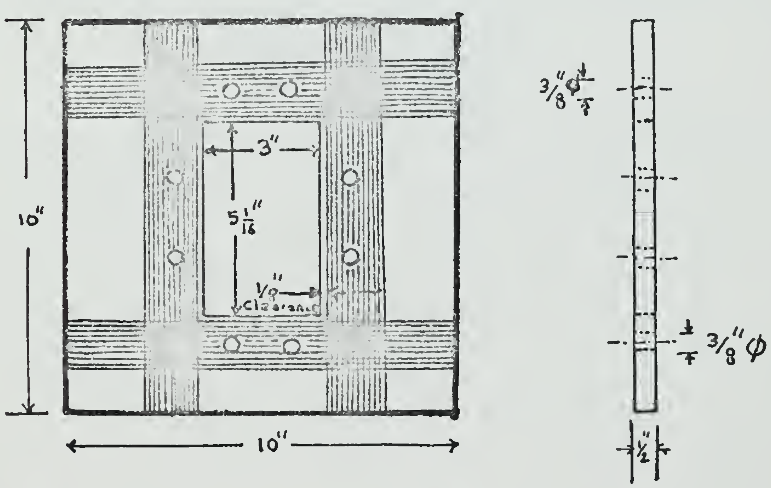

Fig·7 Upper plate

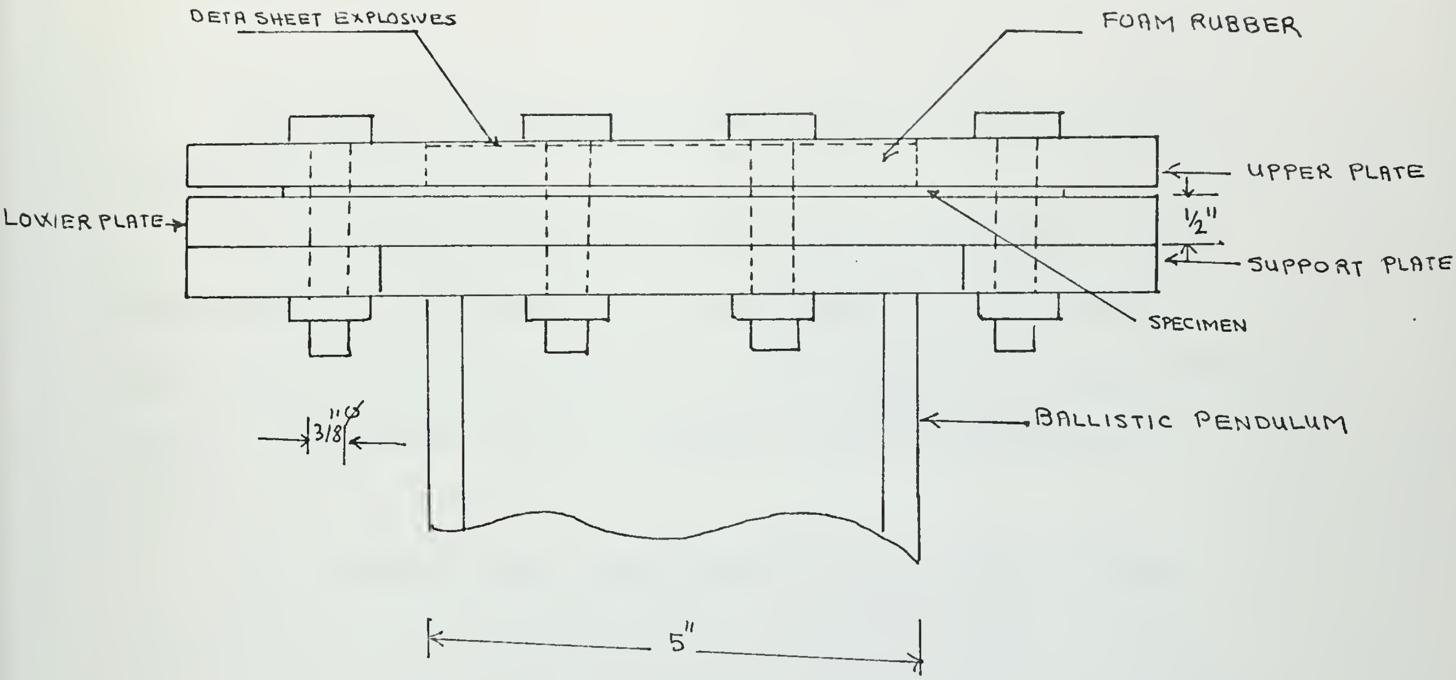

Fig. 8 Location of foam rubber and detasheet

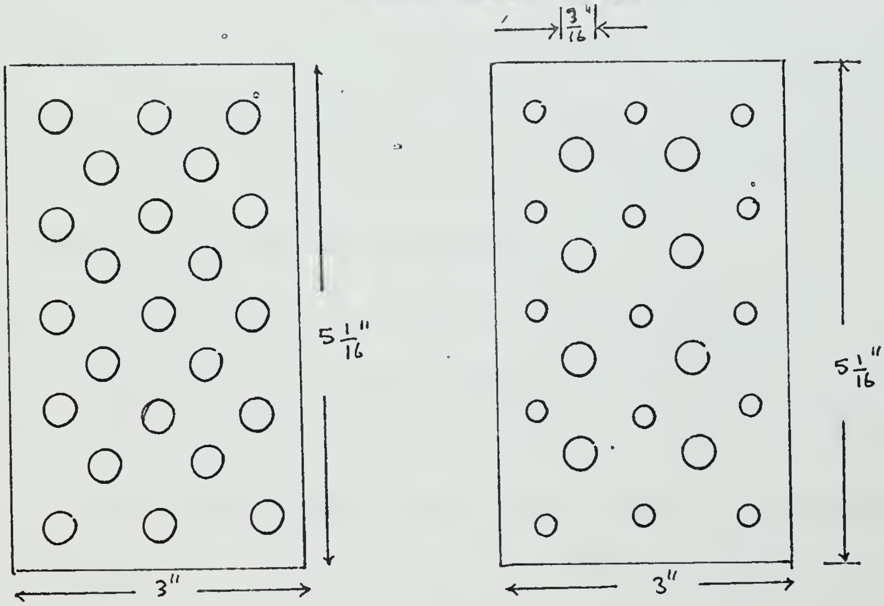

Fig.9 Reduced surface areas of two detasheet explosives

EXPERIMENTAL RESULTS AND DISCUSSION

The results of the experiments are given in Tables (2,3,4) and Fig.(11,12,13,14)

Table (2) and (3) are divided into three categories. The experiments No. 1 to 7 represent thin specimens of $H_1 \cong 0.064$ in., experiments No. 8 to 15 represent the medium specimens of $H_2 \cong 0.098$ in. and the specimens No. 16 to 25 represent the thick specimens of $H_3 \cong 0.173$ in.

The specimens tested using neoprenes have slightly higher deformations than the specimens tested using foam rubbers. However, it is believed that number of experiments performed using neoprenes are not sufficient to drive a general conclusion. The reason for the use of foam rubber instead of neoprene is as follow:

It was not possible to keep the neoprene fixed on the specimen surface. Immediately after the detonation process neoprene moved with an unknown initial velocity in the opposite direction of the ballistic pendulum. It was believed that this undesired motion of neoprene would complicate the calculations.

In all calculations the weight of the neoprene and the foam rubber were neglected. The energy losses due to friction at pivots and the air drag were not taken into account. In the calculations following values of the yield stresses were used. (These average values of yield stresses were obtained from two tensile strength tests for each different plates and the stress - strain curves are presented

in Appendix B).

σ_o = 36598.58 lb/in^2 (for plate of 14 gages)

σ_o = 33787.77 lb/in^2 (" " " 12 Gages)

σ_o = 36007.68 lb/in^2 (" " " 7 Gages)

In the dimensionless parameter, $\lambda = \frac{\mu V_o^2 L^2}{\sigma_o H^3}$ the value of short length of the specimen i.e. 3.0 in. was introduced into notation L. The plates were assumed homogenous and the average density of 0.000732 $\frac{lb-sec}{in^4}$ were used in the calculations.

As indicated in the comment section of Table (II) in a few experiments which were performed with high impulsive loads a slight slip occured and an inclination observed at the boundaries. However, it is shown that these effects were too small to affect the results.

In Fig.(14) the non-dimensionless parameter λ v.s. $\frac{W_{max}}{H}$ appears to represent an excellent illustration of the results. The bending only analysis which has not yet been developed, would be a straight line on this curve and presumable somewhat tangential to the point of this curve near to origin.

Clearly strain rate, strain hardening and finite deflections are extremely important for the large values of the impact velocity, Vo as λ and the bending only analysis would not be sufficient.

TABLE II

Test No.	Specimen No.	Max. Swing (inches)	Distance from Ground (inches)	*Total wgt. of Specimen (Kg.)	Total wgt. of Pendulum (Kg.)	Average Plate Thickness (inches)	Max. Deformation (inches)	$\frac{W_{max}}{H}$	Vo (ft./sec.)	** F or N	Comments
1	70	3.325	7.725	0.393	36.249	0.0643	0.2278	3.542	134.08	F	---
2	9	3.79	7.733	0.385	36.249	0.06443	0.26547	4.120	152.6	F	---
3	10	3.74	7.725	0.389	39.455	0.0638	0.29667	4.65	165.06	F	---
4	8	4.08	7.725	0.384	39.455	0.0638	0.3296	5.166	180.06	F	Slight slip.
5	12	5.816	7.687	0.388	36.250	0.06471	0.4155	6.42	233.0	F	Slip at the holes.
6	80	5.278	7.75	0.395	39.455	0.0635	0.427	6.73	234.08	F	Slip at the holes.
7	11	--	--	--	--	--	--	--	--	N	Experimental error.
8	60	3.15	7.75	0.634	36.549	0.0998	0.1068	1.046	80.735	F	---
9	3	4.15	7.25	0.591	39.460	0.09851	0.18649	1.89	118.95	F	---
10	1	4.68	7.625	0.598	36.460	0.09845	0.1917	1.94	124.2	F	---
11	10	6.09	7.625	0.595	36.460	0.09832	0.270	2.755	161.7	F	---
12	9	6.171	7.725	0.594	39.664	0.09825	0.3278	3.33	177.9	N	---
13	180	7.625	7.805	0.600	36.460	0.0982	0.3695	3.76	202.6	F	---
14	8	8.11	7.512	0.596	36.664	0.09837	0.4068	4.135	216.7	F	Pitted surface
15	2	8.712	7.625	0.595	36.460	0.09843	0.4235	4.30	231.13	F	Slip

TABLE II (Continued)

Test No.	Specimen No.	Max. Swing (inches)	Distance from Ground (inches)	* Total wgt. of Specimen (Kg.)	Total wgt. of Pendulum (Kg.)	Average Plate Thickness (inches)	Max. Deformation (inches)	$\frac{W_{max}}{H}$	Vo (ft./sec.)	** F or N	Comments
16	1	4.50	7.50	1.038	37.2745	0.1728	0.0535	0.3096	69.69	F	---
17	2	5.29	7.50	1.039	40.4795	0.17281	0.089	0.5155	88.858	F	---
18	6	--	7.625	1.040	37.2745	0.17276	0.162	0.9379	--	N	Unballanced swing. (experimental error.)
19	190	7.79	7.750	1.084	40.7595	0.17251	0.1764	1.0225	130.9	F	---
20	100	8.91	7.525	1.085	41.5205	0.17295	0.2175	1.257	153.366	F	---
21	7	9.685	7.750	1.039	41.5205	0.17283	0.244	1.4116	166.26	F	---
22	4	9.91	7.96	1.042	40.4795	0.17292	0.2455	1.420	165.7	N	---
23	5	9.975	7.665	1.040	41.5205	0.1731	0.2734	1.58	171.1	F	---
24	90	9.251	7.625	1.085	46.5218	0.17276	0.2963	1.715	178.02	F	---
25	3	--	7.625	1.0415	51.5205	0.1729	0.4052	2.3433	--	F	No heat-sensitive paper due to large swing.

* Listed values of the specimens are the total weights, i.e. the values of δ x H x 6 x 8 lbs.

** N: Neoprene
F: Foam rubber

TABLE III

Specimen No.	Impact Velocity, Vo (ft. per sec.)	Thickness, H (inches)		WMAX / H
70	134.08	0.0643	112.959	3.542
9	152.6	0.0643	153.273	4.120
10	165.06	0.0638	182.884	4.647
8	180.06	0.0638	217.430	5.166
12	233.0	0.06471	354.245	6.420
80	234.08	0.0635	371.2881	6.730
60	80.735	0.1021	18.500	1.046
3	118.95	0.09851	43.152	1.893
1	124.2	0.09845	47.101	1.947
10	161.7	0.09832	80.052	2.755
9	177.9	0.09825	97.0338	3.336
180	202.6	0.09820	125.977	3.762
8	216.7	0.09837	143.024	4.135
2	231.13	0.09843	163.190	4.302
1	69.69	0.1728	4.532	0.309
2	88.858	0.17281	7.342	0.515
6	------	0.17276	------	0.937
190	130.932	0.17251	15.997	1.022
100	153.366	0.17295	21.837	1.257
7	166.26	0.17283	25.701	1.411
4	165.7	0.17292	25.500	1.420
5	171.1	0.1731	27.132	1.579
90	178.02	0.17276	29.488	1.715
3	------	0.1729	------	2.343

TABLE - IV

TEST NO: 1				TEST NO: 2			
SPECIMEN NO: 70				SPECIMEN NO: 9			
H_1 = 0.0643 in; $\frac{W_m}{H}$ = 3.5427				H_1 = 0.06443 in; $\frac{W_m}{H}$ = 4.12			
POINT NO:	$W \times 10^2$ (inches)	POINT NO:	$W \times 10^2$ (inches)	POINT NO:	$W \times 10^2$ (inches)	POINT NO:	$W \times 10^2$ (inches)
1	0.00	15	19.82	1	0.00	15	22.607
2	9.97	16	11.40	2	12.247	16	14.007
3	17.37	17	0.00	3	20.737	17	0.00
4	21.49	18	0.00	4	24.707	18	0.00
5	22.59	19	9.580	5	26.107	19	11.947
6	22.78	20	15.06	6	26.547	20	18.277
7	22.19	21	17.570	7	26.167	21	21.467
8	20.79	22	18.96	8	24.567	22	22.577
9	17.15	23	0.00	9	19.767	23	0.00
10	9.84	24	6.76	10	11.86	24	8.557
11	0.00	25	9.56	11	0.00	25	11.847
12	0.00	26	9.70	12	0.00	26	13.077
13	11.36	27	11.05	13	13.677	27	13.807
14	19.84			14	22.272		

Continued to Table IV

TEST NO: 3

Specimen No: 10

H_1 = 0.06383 in. ; $\frac{Wm}{H}$ = 4.647

Point No.	W x 10^2 (inches)	Point No.	W x 10^2 (inches)
1	0.0	15	25.337
2	14.427	16	15.147
3	23.507	17	0.0
4	28.367	18	0.0
5	29.667	19	12.767
6	29.647	20	19.897
7	29.137	21	23.797
8	27.467	22	25.307
9	22.487	23	0.0
10	14.037	24	7.869
11	0.0	25	12.537
12	0.0	26	14.737
13	14.967	27	15.107
14	24.767		

TEST NO: 4

Specimen No: 8

H_1 = 0.0638 in. ; $\frac{Wm}{H}$ = 5.16614

Point No.	W x 10^2 (inches)	Point No.	W x 10^2 (inches)
1	0.0	15	28.04
2	14.93	16	17.25
3	24.44	17	0.0
4	30.14	18	0.0
5	32.17	19	14.77
6	32.96	20	21.80
7	32.57	21	26.01
8	30.73	22	27.48
9	24.93	23	0.0
10	15.49	24	10.85
11	0.0	25	14.43
12	0.0	26	16.3
13	15.78	27	17.0
14	27.83		

Continued to Table IV

TEST NO: 5

Specimen No.: 12

H_1 = 0.0647 in.; $\frac{Wm}{H}$= 6.420

Point No.	W x 10^2 (inches)	Point No.	W x 10^2 (inches)
1	0.0	15	35.219
2	19.159	16	21.679
3	32.619	17	0.0
4	39.139	18	0.0
5	41.149	19	17.049
6	41.549	20	27.819
7	41.389	21	32.809
8	38.919	22	34.909
9	31.579	23	0.0
10	18.739	24	11.919
11	0.0	25	17.679
12	0.0	26	20.249
13	21.049	27	21.079
14	35.049		

TEST NO.: 6

Specimen No: 80

H_1 = 0.0635 in.; $\frac{Wm}{H}$= 6.7307

Point No.	W x 10^2 (inches)	Point No.	W x 10^2 (inches)
1	0.0	15	36.10
2	19.14	16	21.9
3	32.29	17	0.0
4	39.37	18	0.0
5	42.34	19	19.27
6	42.74	20	29.38
7	41.27	21	34.37
8	38.3	22	36.03
9	31.87	23	0.0
10	19.67	24	12.44
11	0.0	25	18.54
12	0.0	26	20.53
13	19.33	27	21.38
14	35.84		

Continued to Table IV

TEST NO: 8

Specimen No: 60

H_2 = 0.1021 in.; $\frac{Wm}{H}$ = 1.046

Point No.	W x 10^2 (inches)	Point No.	W x 10^2 (inches)
1	0.0	15	8.9
2	4.71	16	5.04
3	7.81	17	0.0
4	9.98	18	0.0
5	10.66	19	4.40
6	10.68	20	6.91
7	9.79	21	8.20
8	8.74	22	8.68
9	6.52	23	0.0
10	4.17	24	3.08
11	0.0	25	4.18
12	0.0	26	4.88
13	5.17	27	5.04
14	8.46		

TEST NO: 9

Specimen No: 3

H_2 = 0.09851 in.; $\frac{Wm}{H}$ = 1.8931

Point No.	W x 10^2 (inches)	Point No.	W x 10^2 (inches)
1	0.0	15	15.269
2	8.19	16	8.66
3	13.89	17	0.0
4	16.92	18	0.0
5	18.15	19	7.0
6	18.64	20	11.14
7	18.24	21	13.16
8	17.09	22	14.51
9	13.97	23	0.0
10	8.09	24	4.22
11	0.0	25	6.319
12	0.0	26	7.629
13	10.069	27	8.349
14	16.529		

Continued to TABLE - IV

TEST NO: 10 SPECIMEN NO: 1 H_2 = 0.09845 in; $\frac{W_m}{H}$ = 1.94768				TEST NO: 11 SPECIMEN NO: 10 H_2 = 0.09832 in; $\frac{W_m}{H}$ = 2.755			
POINT NO:	$W \times 10^2$ (inches)	POINT NO:	$W \times 10^2$ (inches)	POINT NO:	$W \times 10^2$ (inches)	POINT NO:	$W \times 10^2$ (inches)
1	0.00	15	16.93	1	0.00	15	23.46
2	8.33	16	10.67	2	12.468	16	14.09
3	14.94	17	0.00	3	20.368	17	0.00
4	18.28	18	0.00	4	24.878	18	0.00
5	19.0	19	8.905	5	26.558	19	11.78
6	19.17	20	13.42	6	27.088	20	18.30
7	18.67	21	15.98	7	26.54	21	21.18
8	17.57	22	16.87	8	24.73	22	22.71
9	14.34	23	0.00	9	19.74	23	0.00
10	7.86	24	6.015	10	11.20	24	7.928
11	0.00	25	8.53	11	0.00	25	11.908
12	0.00	26	9.77	12	0.00	26	13.488
13	9.45	27	11.25	13	13.798	27	13.633
14	15.93			14	23.21		

Continued to Table IV

TEST NO: 12

Specimen No: 9

H_2 = 0.09825 in. ; $\frac{Wm}{H}$ = 3.336

TEST NO: 13

Specimen No: 180

H_2 = 0.0982 in. ; $\frac{Wm}{H}$ = 3.7627

POINT NO.	Wx10^2 (inches)	POINT NO.	Wx10^2 (inches)	POINT NO.	Wx10^2 (inches)	POINT NO.	Wx10^2 (inches)
1	0.00	15	28.085	1	0.00	15	31.77
2	16.755	16	16.625	2	16.16	16	18.66
3	27.085	17	0.00	3	27.51	17	0.00
4	31.755	18	0.00	4	33.47	18	0.00
5	32.755	19	16.395	5	36.09	19	14.79
6	32.785	20	22.865	6	36.95	20	23.56
7	31.955	21	25.495	7	36.27	21	28.33
8	29.975	22	27.685	8	34.03	22	30.66
9	24.175	23	0.00	9	27.94	23	0.00
10	14.325	24	9.975	10	15.68	24	9.51
11	0.00	25	12.825	11	0.00	25	14.0
12	0.00	26	15.445	12	0.00	26	16.26
13	16.625	27	16.085	13	18.96	27	17.44
14	27.995			14	32.27		

Continued to Table IV

TEST NO: 14

Specimen No: 2

H_2 = 0.09843in.; $\frac{Wm}{H}$ = 4.303

TEST NO: 15

Specimen No: 8

H_2 = 0.09837 in; $\frac{Wm}{H}$ = 4.1357

POINT NO.	$WX10^2$ (inches)	POINT NO.	$WX10^2$ (inches)	POINT NO.	$WX10^2$ (inches)	POINT NO.	$WX10^2$ (inches)
1	0.00	15	36.757	1	0.00	15	34.463
2	19.477	16	22.157	2	19.288	16	20.443
3	33.207	17	0.00	3	30.993	17	0.00
4	38.982	18	0.00	4	37.463	18	0.00
5	41.577	19	18.877	5	39.818	19	17.643
6	42.357	20	28.407	6	40.683	20	26.603
7	41.257	21	33.347	7	39.513	21	31.383
8	38.477	22	35.137	8	36.933	22	33.273
9	32.877	23	0.00	9	30.503	23	0.00
10	19.60	24	13.167	10	18.443	24	11.713
11	0.00	25	18.217	11	0.00	25	16.483
12	0.00	26	20.267	12	0.00	26	18.382
13	23.187	27	22.027	13	22.143	27	19.753
14	37.137			14	32.413		

Continued to Table IV

TEST NO: 16

Specimen No: 1

H_3 = 0.1728 in. ; $\frac{Wmax}{H}$ = 0.3096

TEST NO: 17

Specimen No: 2

H_3 = 0.17281 in. ; $\frac{Wmax}{H}$ = 0.5155372

POINT NO.	Wx10^2 (inches)	POINT NO.	Wx10^2 (inches)	POINT NO.	Wx10^2 (inches)	POINT NO.	Wx10^2 (inches)
1	0.00	15	4.53	1	0.00	15	7.309
2	2.72	16	3.17	2	4.139	16	5.039
3	3.73	17	0.00	3	6.169	17	0.00
4	4.57	18	0.00	4	7.559	18	0.00
5	5.12	19	2.645	5	8.499	19	4.119
6	5.35	20	3.47	6	8.909	20	5.669
7	5.07	21	4.06	7	8.459	21	6.569
8	4.5	22	4.52	8	7.619	22	7.239
9	3.54	23	1.74	9	6.109	23	0.00
10	2.6	24	2.25	10	4.309	24	3.109
11	0.00	25	2.71	11	0.00	25	3.919
12	0.00	26	3.09	12	0.00	26	4.739
13	3.03	27	3.17	13	4.929	27	5.141
14	4.35			14	7.409		

Continued to Table IV

TEST NO.: 18

Specimen No.: 6

H3 = 0.1726 in.; $\frac{Wm}{H}$ = 0.9379

TEST NO.: 19

Specimen No. = 190

H3 = 0.17251 in.; $\frac{Wm}{H}$ = 1.02249

Point No.	W x 10^2 (inches)	Point No.	W x 10^2 (inches)	Point No.	W x 10^2 (inches)	Point No.	W x 10^2 (inches)
1	0.0	15	13.574	1	0.0	15	14.679
2	6.114	16	7.904	2	6.929	16	8.349
3	10.774	17	0.0	3	12.269	17	0.0
4	13.444	18	0.0	4	15.759	18	0.0
5	15.374	19	5.354	5	17.219	19	6.399
6	16.204	20	8.734	6	17.639	20	10.949
7	15.694	21	10.774	7	16.309	21	13.33
8	14.354	22	12.114	8	13.999	22	14.559
9	11.154	23	0.0	9	9.959	23	0.0
10	6.224	24	3.474	10	5.829	24	4.429
11	0.0	25	5.294	11	0.0	25	6.529
12	0.0	26	6.404	12	0.0	26	7.799
13	6.824	27	7.114	13	8.699	27	8.339
14	12.954			14	14.339		

Continued to TABLE - IV

TEST NO: 20
SPECIMEN NO: 100
H_3 = 0.17295 in; $\frac{W_m}{H}$ = 1.275

POINT NO:	W x 10^2 (inches)	POINT NO:	W x 10^2 (inches)
1	0.00	15	17.855
2	7.705	16	10.055
3	14.505	17	0.00
4	19.105	18	0.00
5	21.655	19	7.035
6	21.75	20	12.655
7	21.255	21	15.905
8	18.705	22	16.855
9	14.505	23	0.00
10	7.655	24	4.595
11	0.00	25	7.525
12	0.00	26	9.005
13	10.535	27	9.346
14			

TEST NO: 21
SPECIMEN NO: 7
H_3 = 0.17283 in; $\frac{W_m}{H}$ = 1.41161

POINT NO:	W x 10^2 (inches)	POINT NO:	W x 10^2 (inches)
1	0.00	15	19.867
2	9.307	16	11.017
3	16.617	17	0.00
4	21.217	18	0.00
5	23.607	19	8.207
6	24.397	20	13.817
7	23.347	21	17.037
8	20.747	22	18.437
9	15.977	23	0.00
10	9.027	24	5.347
11	0.00	25	8.377
12	0.00	26	9.787
13	11.717	27	10.507
14	19.817		

Continued to Table IV

TEST NO: 22

Specimen No: 4

$H_3 = 0.17292$ in. ; $\frac{Wm}{H} = 1.4201$

POINT NO.	$Wx10^2$ (inches)	POINT NO.	$Wx10^2$ (inches)
1	0.00	15	20.398
2	8.838	16	11.408
3	15.308	17	0.00
4	20.468	18	0.00
5	23.118	19	7.958
6	24.558	20	13.738
7	23.908	21	17.818
8	21.458	22	19.588
9	16.358	23	0.00
10	9.558	24	4.943
11	0.00	25	8.288
12	0.00	26	10.008
13	11.288	27	11.088
14	20.028		

TEST NO: 23

Specimen No: 5

$H_3 = 0.17310$ in. ; $\frac{Wm}{H} = 1.57943$

POINT NO.	$Wx10^2$ (inches)	POINT NO.	$Wx10^2$ (inches)
1	0.00	15	22.65
2	10.66	16	12.56
3	19.055	17	0.00
4	23.92	18	0.00
5	26.44	19	10.17
6	27.34	20	16.57
7	26.59	21	19.84
8	24.07	22	22.10
9	19.45	23	0.00
10	10.99	24	6.58
11	0.00	25	9.64
12	0.00	26	11.79
13	13.14	27	12.54
14	22.71		

Continued to Table IV

ST NO.: 24 | TEST NO.: 25

pecimen No.: 90 | Specimen No.: 3

3 = 0.17276 in.; $\frac{W_m}{H}$ = 1.715 | H3 = 0.1729 in.; $\frac{W_m}{H}$ = 2.343

oint No.	W x 10^2 (inches)	Point No.	W x 10^2 (inches)	Point No.	W x 10^2 (inches)	Point No.	W x 10^2 (inches)
1	0.0	15	23.274	1	0.0	15	34.36
2	11.244	16	14.184	2	18.20	16	19.88
3	19.814	17	0.0	3	29.80	17	0.0
4	25.344	18	0.0	4	36.49	18	0.0
5	28.344	19	10.314	5	39.67	19	15.83
6	29.634	20	16.484	6	40.52	20	25.32
7	28.844	21	20.854	7	39.49	21	30.06
8	25.874	22	22.904	8	36.01	22	32.98
9	20.574	23	0.0	9	30.01	23	0.0
10	12.034	24	6.144	10	17.81	24	9.86
11	0.0	25	9.804	11	0.0	25	14.65
12	0.0	26	11.734	12	0.0	26	17.4
13	17.504	27	13.294	13	20.49	27	19.12
14	15.276	[illegible]		14	34.77		

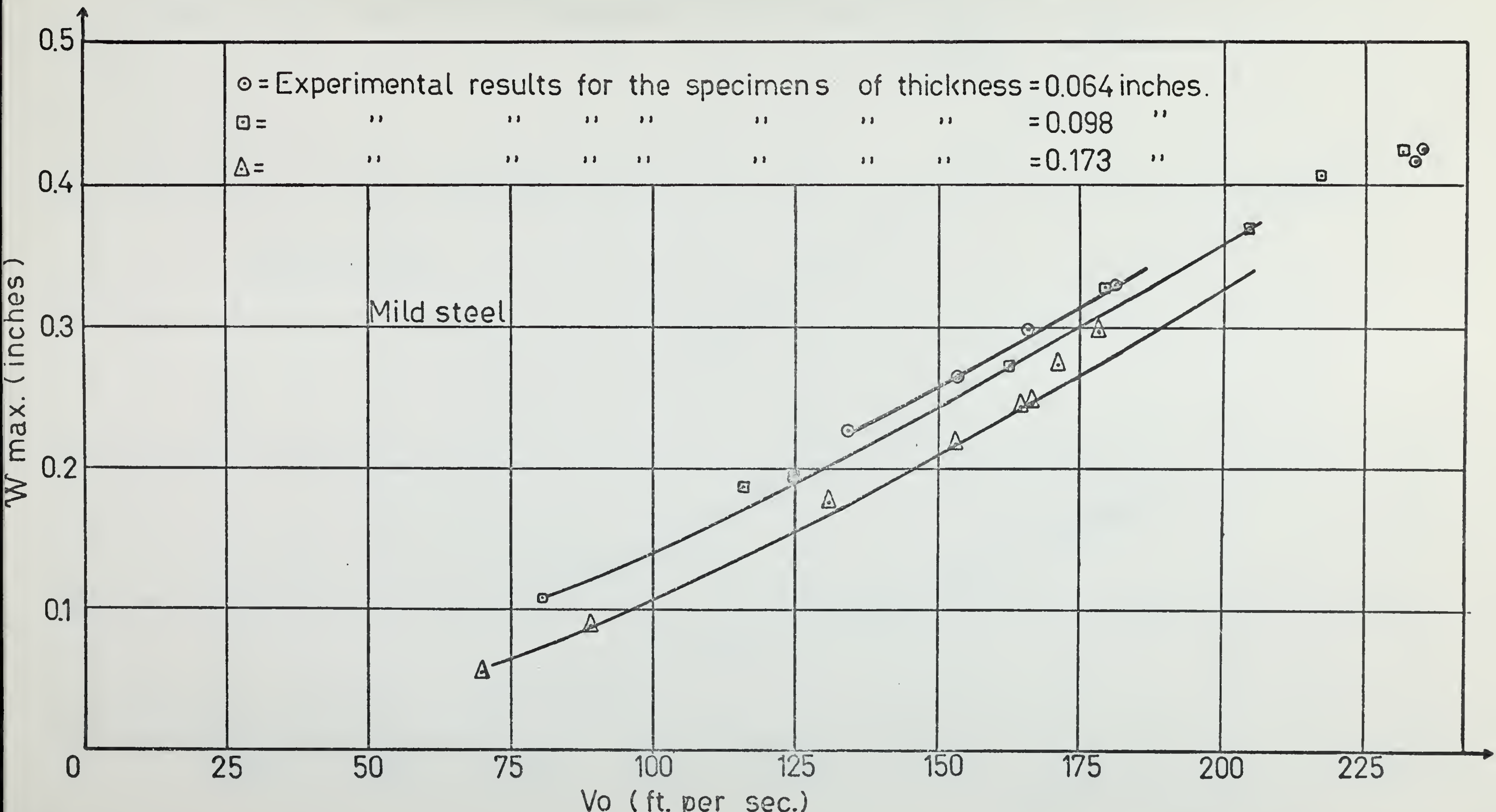

FIG. 11 MAXIMUM DEFORMATION VERSUS IMPACT VELOCITY

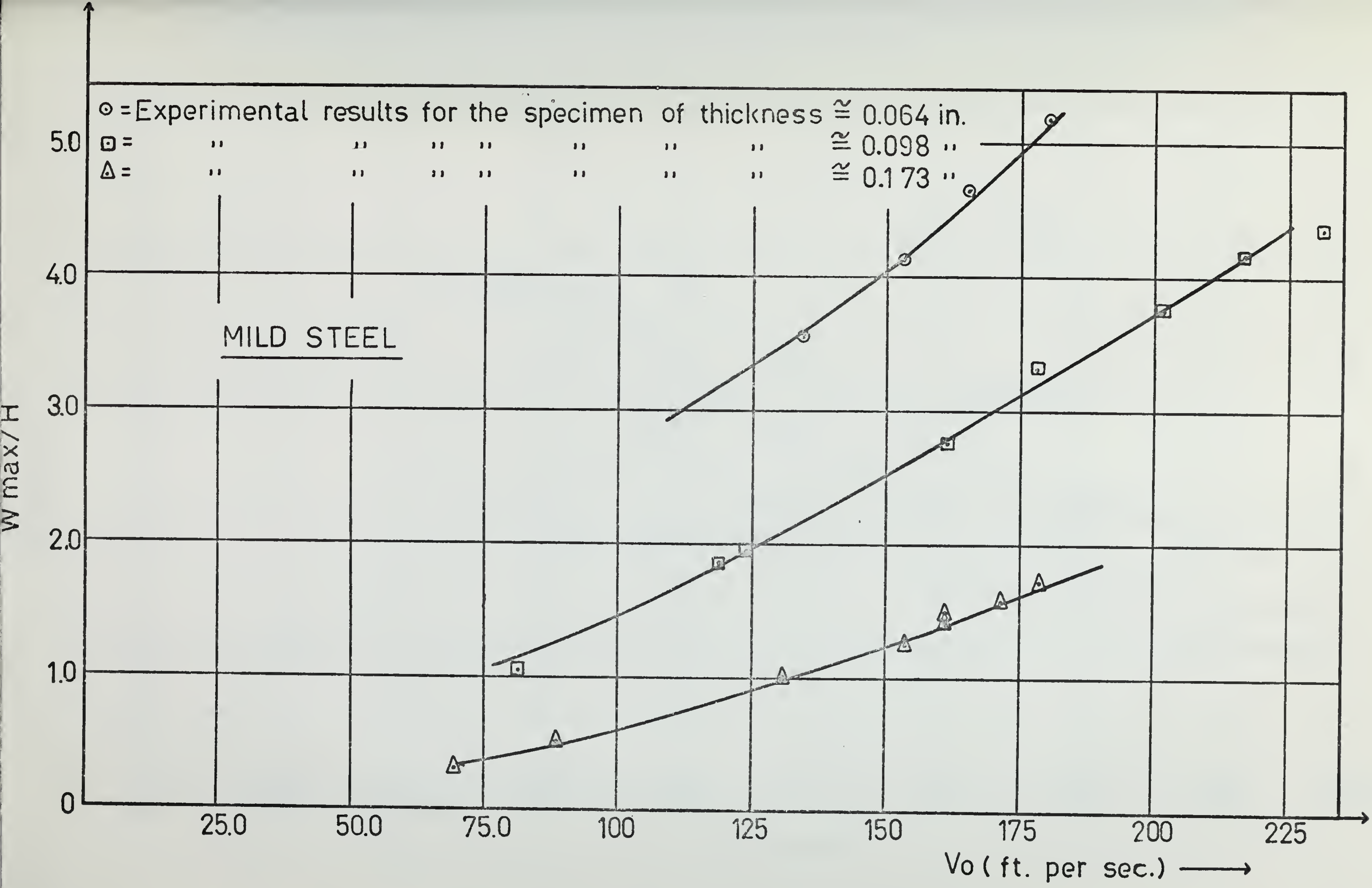

FIG. 12. DIMENSIONLESS DEFORMATION VERSUS IMPACT VELOCITY.

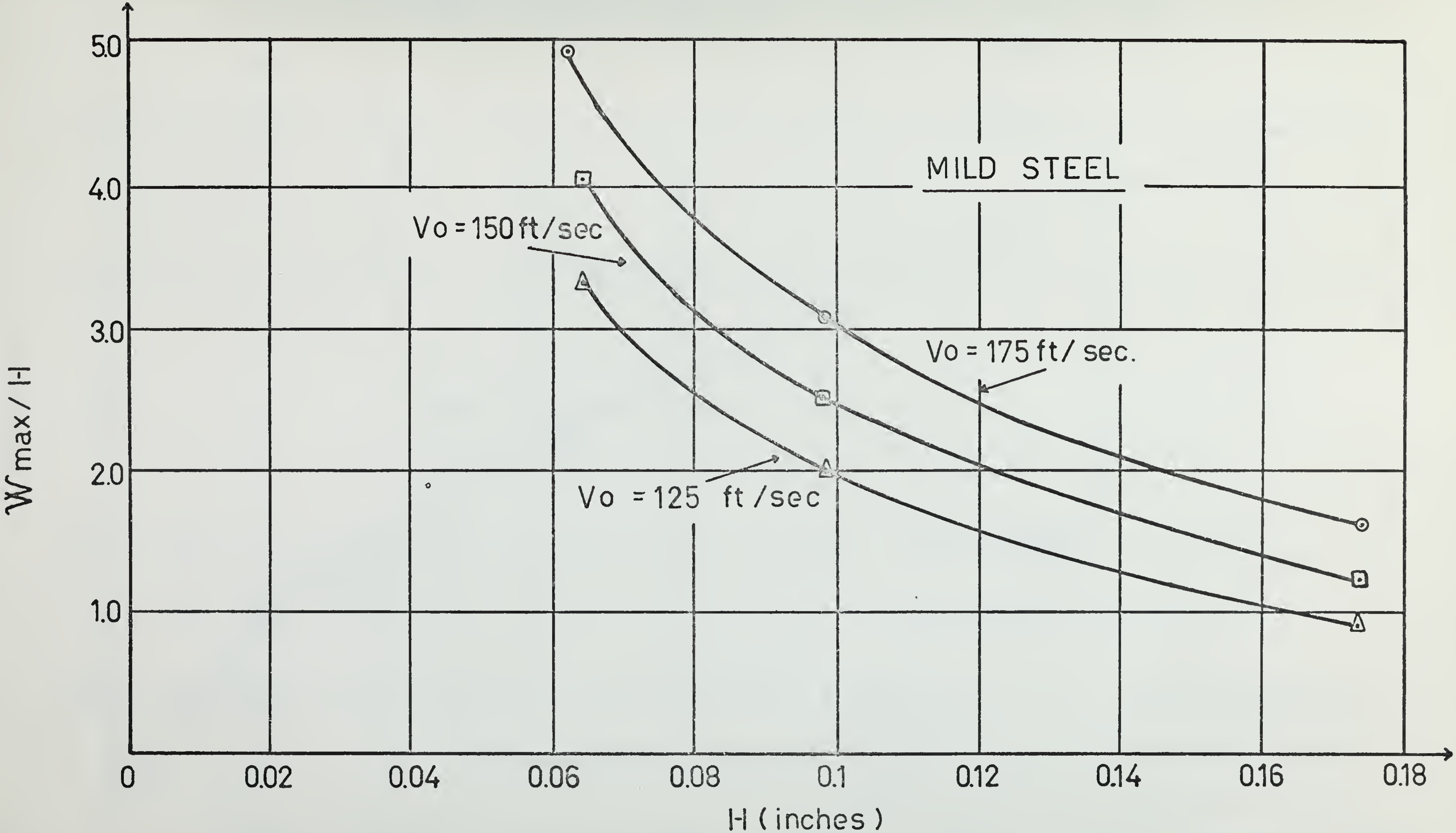

FIG.13. PLATE THICKNESS, H VERSUS DIMENSIONLESS DEFORMATION, Wmax/H (CONSTANT V

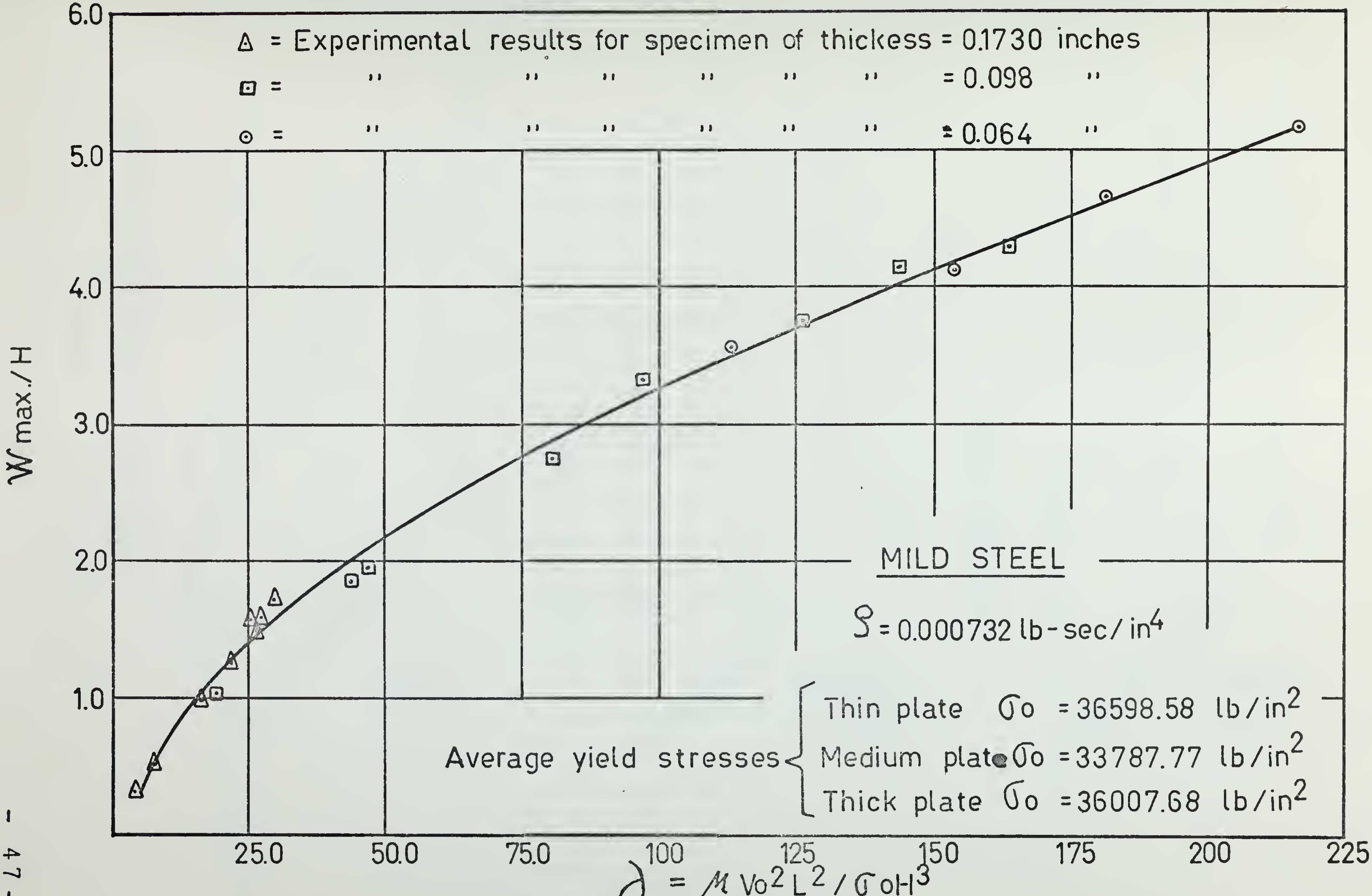

FIG. 14. DIMENSIONLESS DEFORMATION VERSUS DIMENSIONLESS λ

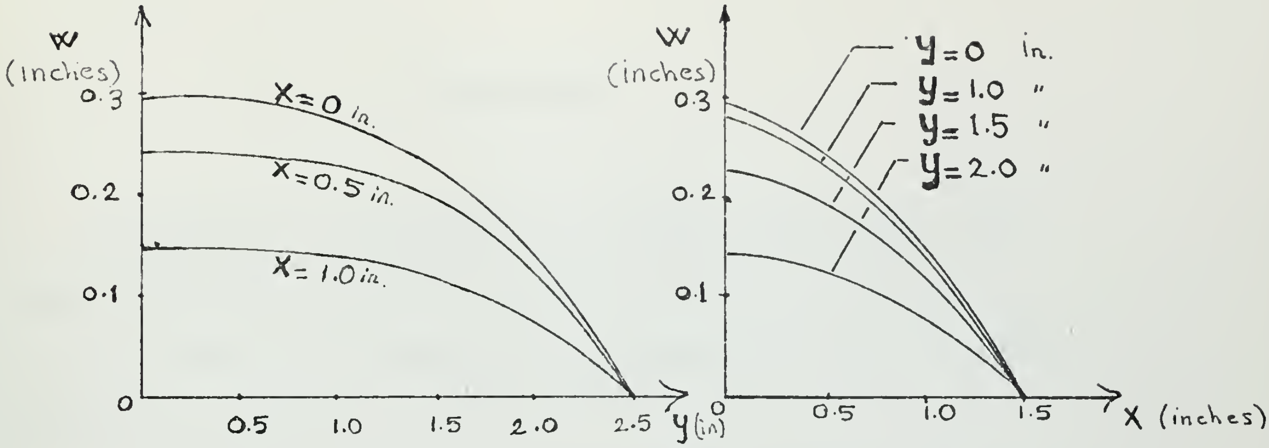

Test No: 3

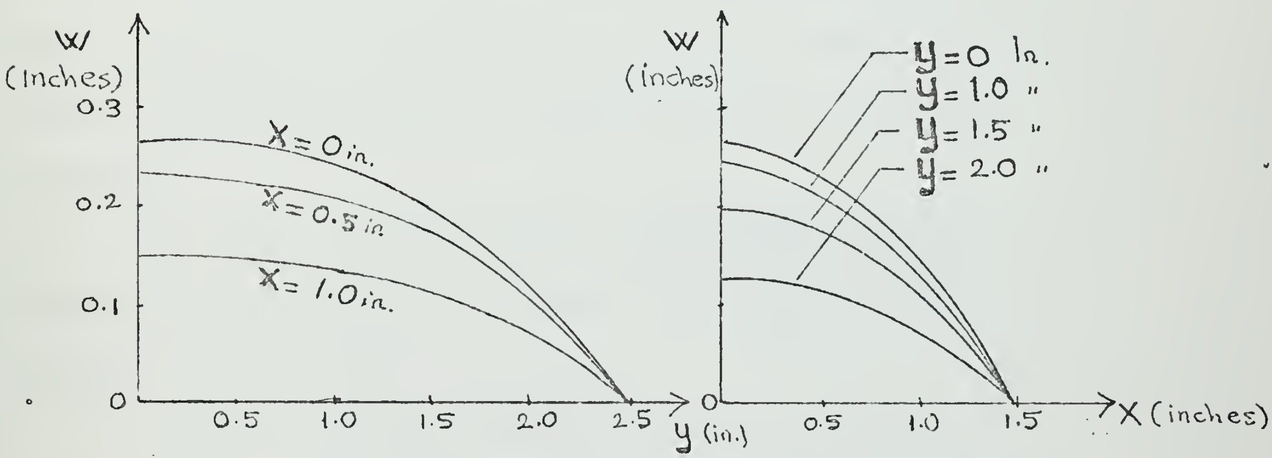

Test No: 11

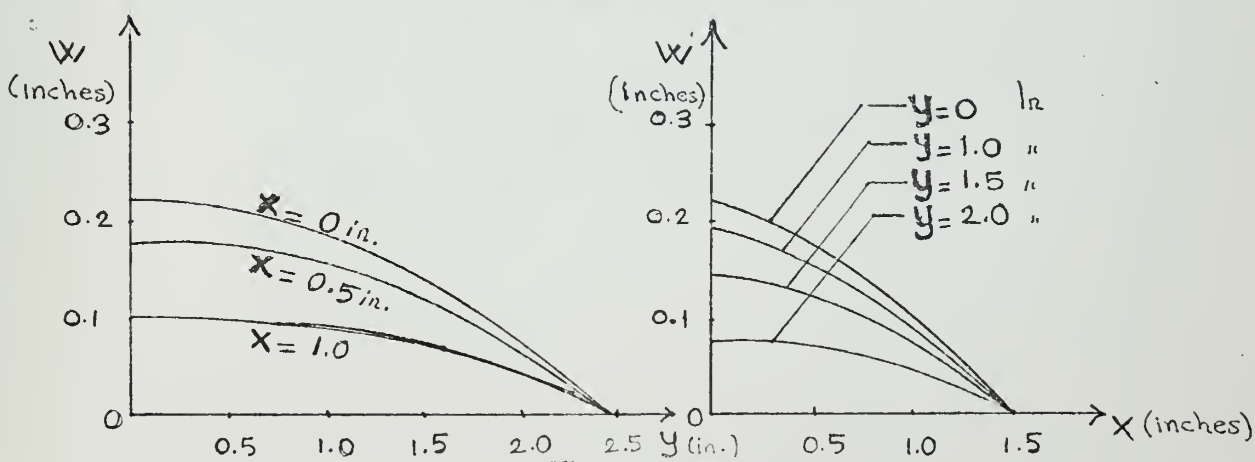

Test No: 20

Deformation profiles

(refer to Table-4)

CONCLUSIONS

The behaviour of rectangular, mild steel plates with four edges clamped when subjected to uniform impulsive loads are studied herein and the results are presented in Fig.(11,12,13,14) and Tables (2,3,4).

It is shown from Fig.(14) that strain hardening, strain rate and finite deflections are extremely important for large values of impact velocity and therefore the bending only analysis would not provide a sufficient answer for the large values of the impact velocity.

It is also concluded that high temperatures caused by detasheet explosition would not create any thermal stresses or thermal shock problems.

Although the study can not be considered complete, it is believed that a reasonable number of useful results are presented to aid the development of future theoretical studies.

RECOMMENDATIONS

1. For higher values of the impact velocity, a bigger number of bolts is required to maintain the boundary conditions fix.

2. To prevent deformation and improve rigidity, thicknesses of the lower and upper heads should be increases.

3. An increase in the number of tensile strength tests will yield more accurate value for the yield stress.

4. In the chemical analysis of the samples taken from a plate, the following suggestion is presented.

After the analysis of the total content of the plate, take more samples from the same plate and analyze each individual sample for its alloying elements which have dominate effect on the mechanical properties of the material. For example, in mild steel, analyze only Carbon and Phosphore.

5. Increase weight of ballistic pendulum for experiments with thicker plates, so as to decrease the max swing angle or modify the "heat sensitive paper device" to allow for recording of larger displacements. However, this involves the difficulty of ballancing the ballistic pendulum at high impact velocities.

APPENDIX A

"THE RESULTS OF CHEMICAL ANALYSIS"

Alloying elements of the three mild steel plates of 14 gages, 12 gages and 7 gages were analyzed at the "Central Analytical Laboratory" at the Massachusetts Institute of Technology. The original copy of the report is attached to the Appendix.

It is shown that the percentages of the carbon content vary widely. The percentage difference of the carbon content between the plate of 14 gages and the plate of 12 gages is about 87 percent.

MASSACHUSETTS INSTITUTE OF TECHNOLOGY

DEPARTMENT OF METALLURGY

CENTRAL ANALYTICAL LABORATORY

Report of Chemical Analysis

To: Sedat Tekin

Charged to: 27703

Description of Samples: Al 6061 and Mild Steel

Received: April 17, 1969

Reported: May 1, 1969

Notebook No. 132 Page: 132, 134

137 2, 8

136 15

Weight Per Cent Unless Noted Otherwise

	Sample	% Si	% Cu	% Mg	% Cr			
Al	11/1/8	0.65	0.20	0.85	0.26			
	11/.193	0.61	0.21	0.83	0.21			
	13/.09	0.57	0.24	0.89	0.23			
		% C	% Mn	% P	% S	% Si		
Steel	T1	0.071	0.41	0.008	0.021	0.001		T1 = 7 Gages
	T2	0.046	0.25	0.007	0.019	0.001		T2 = 12 Gages
	T3	0.086	0.34	0.009	0.023	0.003		T3 = 14 Gages

Copies to:

Reported by: Donald L. Guernsey

APPENDIX B

TENSILE STRENGTH TEST RESULTS

The tensile strenght tests were performed for each different plate thickness, i.e., 14 gages, 12 gages and 7 gages. The stress-strain curves of the plates are attached to the Appendix.

In Figure 15, the plots verify the report of chemical analysis of the plates. The relatively high yield strength of the specimens cut from the plate of 14 gages is due to the higher carbon content of these specimens. Ref.(19).

An exact evaluation of the yield stresses however, requires a greater number of tensile strength tests.

From Figure 15 the following results were obtained and used in the calculations:

(σ_o) average = 36.598 p.s.i. for the plate of 14 gages
(σ_o) average = 33.787 p.s.i. for the plate of 12 gages
(σ_o) average = 36.0068 p.si. for the palte of 7 gages.

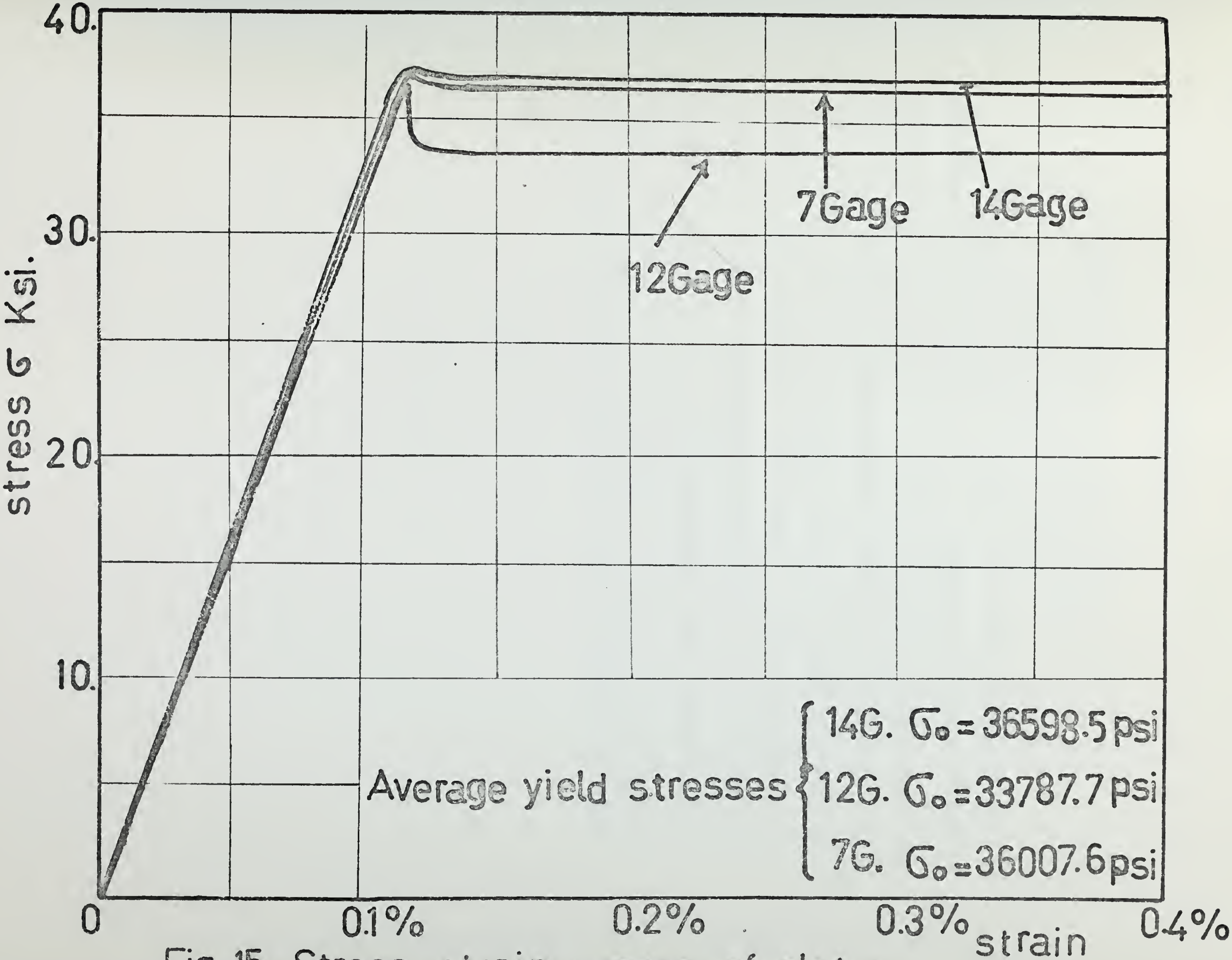

Fig. 15. Stress strain curves of plates

APPENDIX C

COMPUTER RESULTS OF IMPACT VELOCITY, Vo AND APPROXIMATE VALUES OF Vo

In this Appendix computer results of the impact velocities are presented. The notations "Vel" and "A" represent the impact velocities computed using Equation 3 and 4 on Page 16, respectively. It is shown that the assumptions of $m \ll M$ and $R \cong R^*$ create an error less than 0.16%.

It is concluded that up to 250 ft. per sec. impact velocity may be calculated using Equation 4. It is clear that this conclusion is not a general one, when R, R* decrease or/and (R-R*) and M increase, then Equation 4 may not be used. The calculations must be performed by a computer otherwise about 5% error may be involved in the calculations due to rough interpolated cosine values given in mathematical tables.

```
C     SEDAT TEKIN,THESIS STUDY, 1969
C     IMPACT VELOCITIES OF THE SPECIMENS
 50   READ(8,4) N,W,H,S,D,CGS
 4    FORMAT(I5,5F10.5)
      WSP=1.9412525*H
      SCG=136.3-D
      PCG=SCG-CGS
      V=W*PCG**2+WSP*SCG**2
      ACI=S/133.55
      BACI=ACI/2.
      A=SQRT(1.-COS(ACI))
      VEL=SQRT(772.146*V*PCG*W)*A/(12.*WSP*SCG)
      AVEL=SQRT(386.*V*W/SCG)*(SIN(BACI))*2./(12.*WSP)
      WRITE (5,2)  N, VEL, AVEL
      IF (N-190) 50,51,50
 2    FORMAT(5X,' N=',I5,' VEL=',F20.10,' A=',F10.5)
 51   CALL EXIT
      END
```

N=	70	VEL*=	134.0963444113	A**=	134.19839
N=	10	VEL=	165.0748294591	A=	165.32000
N=	80	VEL=	234.0378116965	A=	234.39666
N=	12	VEL=	233.0739750266	A=	233.27319
N=	8	VEL=	180.0824588537	A=	180.34799
N=	9	VEL=	152.5960392355	A=	152.72290
N=	11	VEL=	272.2458503246	A=	272.66034
N=	60	VEL=	80.7389070391	A=	80.80232
N=	3	VEL=	118.9668428301	A=	119.14300
N=	1	VEL=	124.2385255694	A=	124.34207
N=	9	VEL=	178.0052798986	A=	178.27883
N=	10	VEL=	161.7769474387	A=	161.91061
N=	180	VEL=	202.6026920080	A=	202.77401
N=	2	VEL=	231.1393436789	A=	231.33258
N=	8	VEL=	216.7216495871	A=	216.90469
N=	1	VEL=	69.6988527476	A=	69.74987
N=	2	VEL=	88.8603212237	A=	88.99168
N=	7	VEL=	166.2684635519	A=	166.55499
N=	100	VEL=	153.3670963644	A=	153.63281
N=	90	VEL=	178.0288089513	A=	178.38232
N=	5	VEL=	171.1031192541	A=	171.39953
N=	4	VEL=	165.7430118322	A=	166.03027
N=	190	VEL=	130.7073367834	A=	130.93283

*VEL = Impact Velocity (ft/sec) (From equation 3)

**A = Impact Velocity (ft/sec) (From equation 4)

APPENDIX D

MECHANICAL PROPERTIES OF FOAM RUBBER AND NEOPRENE

In this Appendix properties of neoprene and foam rubber are presented for future studies. Properties have been given in Ref. (17) and (18).

TABLE - V

PROPERTIES OF NEOPRENE*

Property		Unvulcanized	Ref.	Pure-gum Vulcanizate	Ref.	Vulcanizate Containing About 33% Carbon Black (~50 phr)
Density	[g cm^{-3}]	1.23	4,12,36	1.32	14	1.42
Coefficient of Expansion, volume (1/V(dV/dT)	[(deg C)$^{-1}$]	60 x 10^{-5}	4,8	61-72 x 10^{-5}	4,14	
Thermal						
Glass Transition Temperature	[deg C]	-45	22	-44	22,38	-43
Specific Heat	[cal g^{-1}(deg C)$^{-1}$]	0.52	4	0.49-0.52	8	0.40-0.42
Thermal Conductivity		46 x 10^{-5}	4	46 x 10^{-5}	8,34	50 x 10^{-5}
Optical						
Refractive Index n_D		1.558	11			----
dn_D/dT	[(deg C)$^{-1}$]	-36 x 10^{-5}	11			----
Electrical						
Dielectric Constant (1 kc)				6.5-8.1	7	
Dissipation Factor (1 kc)				0.031-0.086	7	
Conductivity	[mho cm^{-1}]			3-1400 x 10^{-14}	7	
Mechanical						
Compressibility B	[bar^{-1}]	48 x 10^{-6}	15,25	44 x 10^{-6}	15,25	36 x 10^{-6}
dB/dP	[bar^{-2}]	-0.028 x 10^{-6}	25	-0.023 x 10^{-6}	25	-0.017 x 10^{-6}
Bulk Wave Velocity v_b	[m sec^{-1}]			1420	15	1520
Strip (longitudinal wave) Velocity v_1 (1 kc)	[m sec^{-1}]			69	8,15	196
Ultimate Elongation	[%]	----		800-1000	1.2	500-600
Tensile Strength	[kg cm^{-2}]	----		250-375	1,2	210-300
Initial Slope of Stress-Strain Curve Young's Modulus E (1 min.)	[dyne cm^{-2}]	----		16 x 10^{6} (10-30 x 10^{6})	23.38 2.23.38	30-50 x 10^{6}
Shear Modulus G (1 min.)	[dyne cm^{-2}]	----		5.2 x 10^{6} (3-10 x 10^{6})	38 2.23.28	14 x 10^{6}
Shear Compliance J (1 min.)	[cm^{2} (dyne)$^{-1}$]	----		0.20 x 10^{-6} (0.1-0.3 x 10^{-6}	38 2,23, 38	0.07 x 10^{-6}
Creep (1/J)(dJ/d log t)	[% (decade)$^{-1}$]	----		6 (5-10)	23.38 23.38	
Complex Dynamic Shear Modulus G* (60 cycles)						
Storage Modulus G' (Values of log G')	[dyne cm^{-2}]			6.81	17	7.45
Loss Modulus G" (Values of log G")	[dyne cm^{-2}]			6.04	17	6.75
Loss Tangent G"/G;				0.17	17	0.20
Resilience (rebound)	[%]			60-65	2,16	48 (40-50)

* FROM REF.(17)

TABLE – V (Continued)

PROPERTIES OF FOAM RUBBER **

Plastic Composition	Polystyrene						Polyurethane			Epoxy	Phenol-formaldehyde			Polyethylene			Urea-formaldehyde	Silicone		Cellulose acetate
	Extruded			Molded			Polyether Board	Polyether FIP[e]	Polyester FIP[e]											
Density, lb/ft³:	1.9	2.9	4.4	1.0	2.0	4.0	2.3	2.5	2.1	2.3	2.0	4.0	8.0	2.0	29[f]	30[g]	1.8	3.5	14	6 7
Mechanical Properties at 75°F																				
Compressive strength, psi	35	65	130	20	35	70	50[a]	32	37	25	25	55	140				8	6.2	200	125
Tensile strength, psi	70	105	178	20	45	85		30	47	40	15	30	70	25	670	1800				170
Flexural strength, psi	70	80	160	20	60	120	60	55	60		45	90	205				17			147
Shear strength, psi	40	58	88				30[b]					25	45							140
Compressive modulus, psi × 10³	1.0	3.0	5.05	.25	.75	1.75	1.0[a]			.57										
Flexural modulus, psi × 10³	2.5	2.0	2.95	2.0	2.4	6.6	1.0										.7			
Shear modulus, psi × 10³	.9	1.8	2.95				.5[b]													
Thermal Properties																				
Thermal conductivity (initial), Btu-in. °F⁻¹ft⁻²hr⁻¹	.26			.16	.16	.16	.12	.110	.110	.11								.281	.3	
Thermal conductivity (equil.), Btu-in. °F⁻¹ft⁻²hr⁻¹	.26			.260	.240	.243	.165	.150	.157	.15	.20	.20	.27	.035			.23			.31
Coefficient of thermal expansion, in. in.⁻¹ °F⁻¹ × 10⁻⁴	3.5			3.3 to 3.5			2.7				1-3	1-3	1-3							2.5
Flammability[h]	burns—can be made FR										FR	FR	FR	burns			FR	FR		burns
Heat distortion temp., °F	170	170	170	175	175	175	250			300	250			160			120	650	700	350
Electrical Properties																				
Dielectric constant at 10⁶cps	<1.05	1.07	1.07	<1.017	1.03	1.06	1.04							1.05	1.50	1.55		1.09	1.25	1.12
Dissipation factor at 10⁶cps, × 10⁻⁴	<4.0	<4.0	<4.0	<1.0	7.0		13							2.0	3.3	40.0			10.2	20
Chemical Properties																				
Water absorption (10-ft head), lb/ft²	.08	.08	.08	nil	nil	nil	<.04	.06	.04	.03				.4				.284		
Water absorption, vol.%				<1.0	<1.0	<1.0	<2.0				100			4.0					2.3	4.5
Moisture-vapor transmission, perm-inch	1.5	1.5	1.5	2.0	2.0	2.0	<2.5	1.7	1.0	1	.4[c] / 21[d]							41.2		
Specific heat, Btu/lb	.29										.38	.38	.38				.40			

a. Load parallel to thickness dimension.
b. Load perpendicular to thickness dimension.
c. With skin.
d. Without skin.
e. FIP = foamed-in-place.
f. Prepared from low-density polyethylene.
g. Prepared from high-density polyethylene.
h. FR = flame retardant.

** From Ref.(18)

APPENDIX E

LOCATIONS OF THE SPECIMENS ON THE ORIGINAL PLATES

In this Appendix the locations of the specimens on the plates are presented by Fig.(16-a) and (16-b).

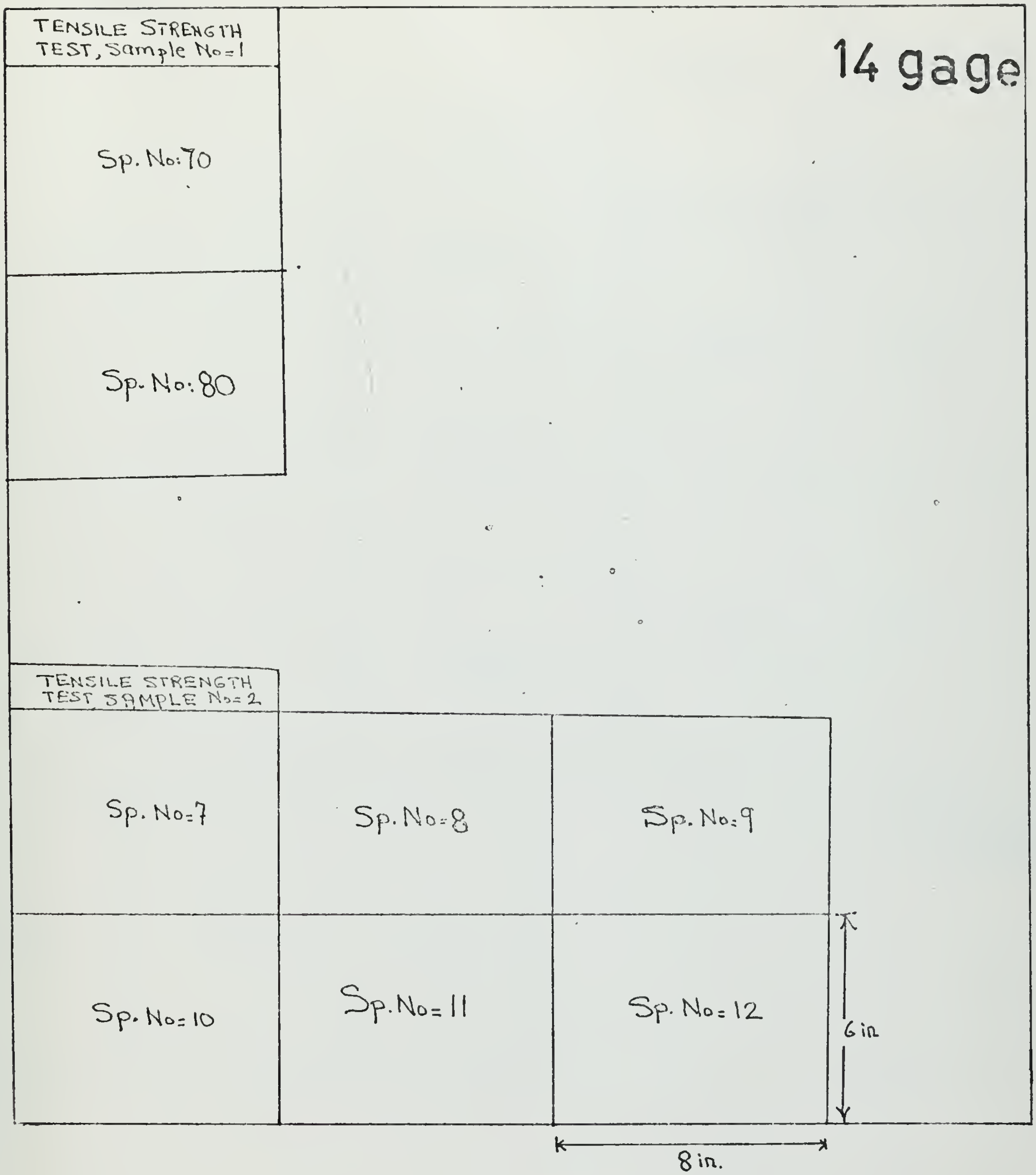

14 gage
TENSILE STRENGTH TEST, Sample No=1
Sp. No:70
Sp. No:80
TENSILE STRENGTH TEST SAMPLE No=2
Sp. No=7
Sp. No=8
Sp. No=9
Sp. No=10
Sp. No=11
Sp. No=12
6 in
8 in.

Fig.16-a

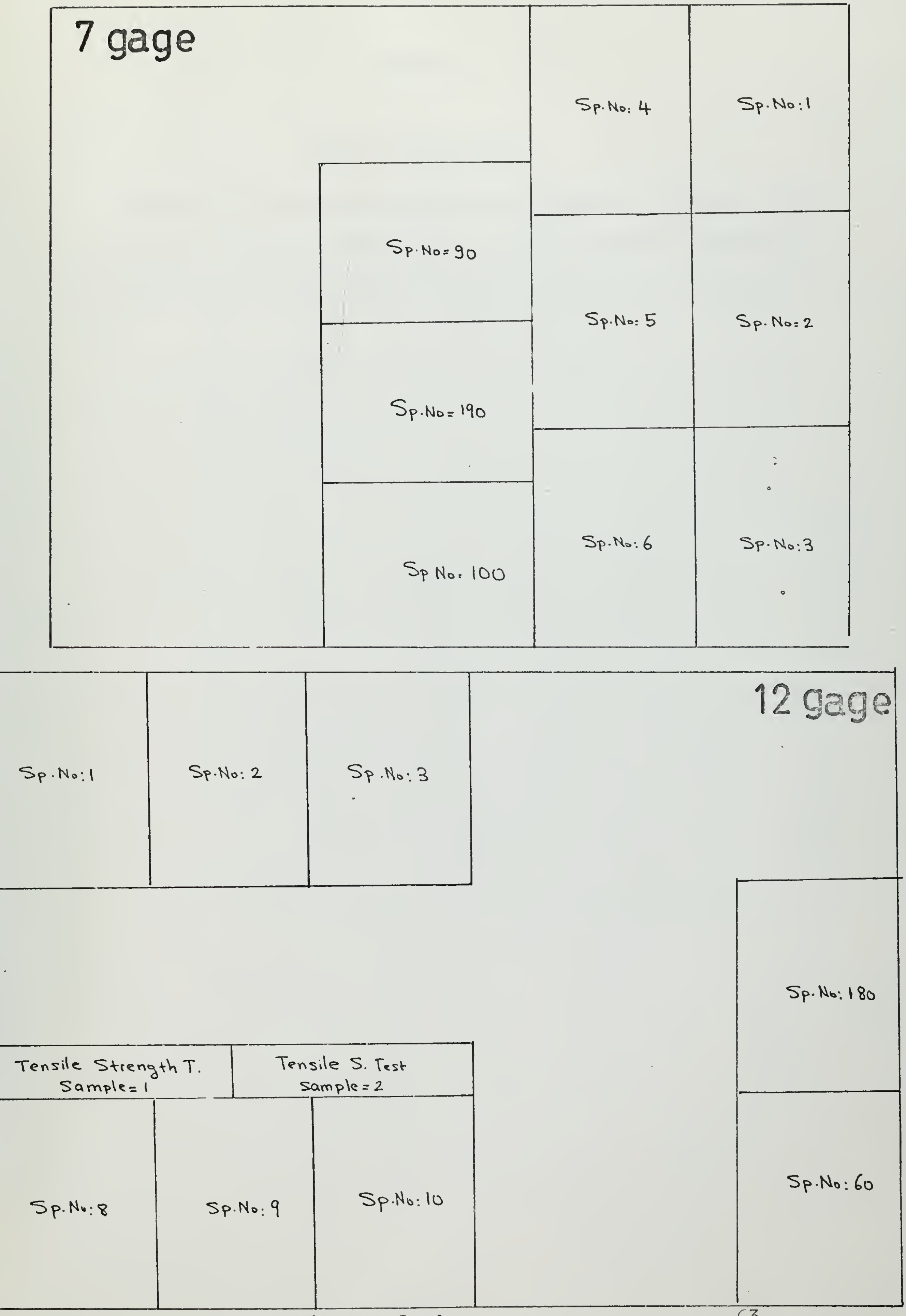
7 gage
Sp. No: 4
Sp. No: 1
Sp. No= 90
Sp. No: 5
Sp. No: 2
Sp. No= 190
Sp. No: 6
Sp. No: 3
Sp No: 100
12 gage
Sp. No: 1
Sp. No: 2
Sp. No: 3
Sp. No: 180
Tensile Strength T. Sample = 1
Tensile S. Test Sample = 2
Sp. No: 8
Sp. No: 9
Sp. No: 10
Sp. No: 60

Fig.16-b

APPENDIX F

PLAN OF THE CHAMBER

The plan of the chamber was reproduced from the original plan and presented in the following page. Chamber in which experiments were carried out was denoted with the "blast tank" on the original plan.

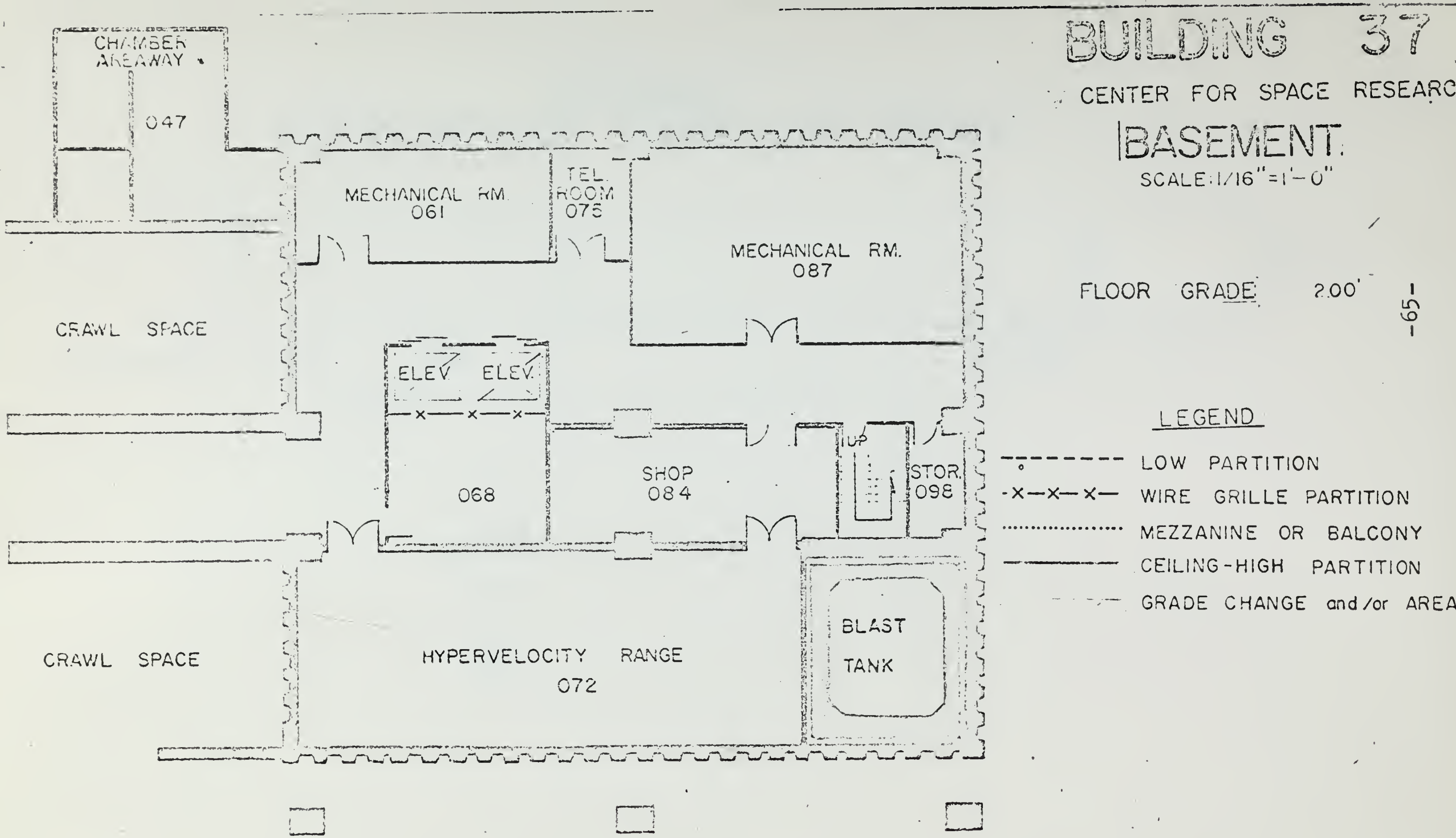

Fig.17 (Plan of the Chamber)*

* REPRODUCED FROM THE ORIGINAL PLAN

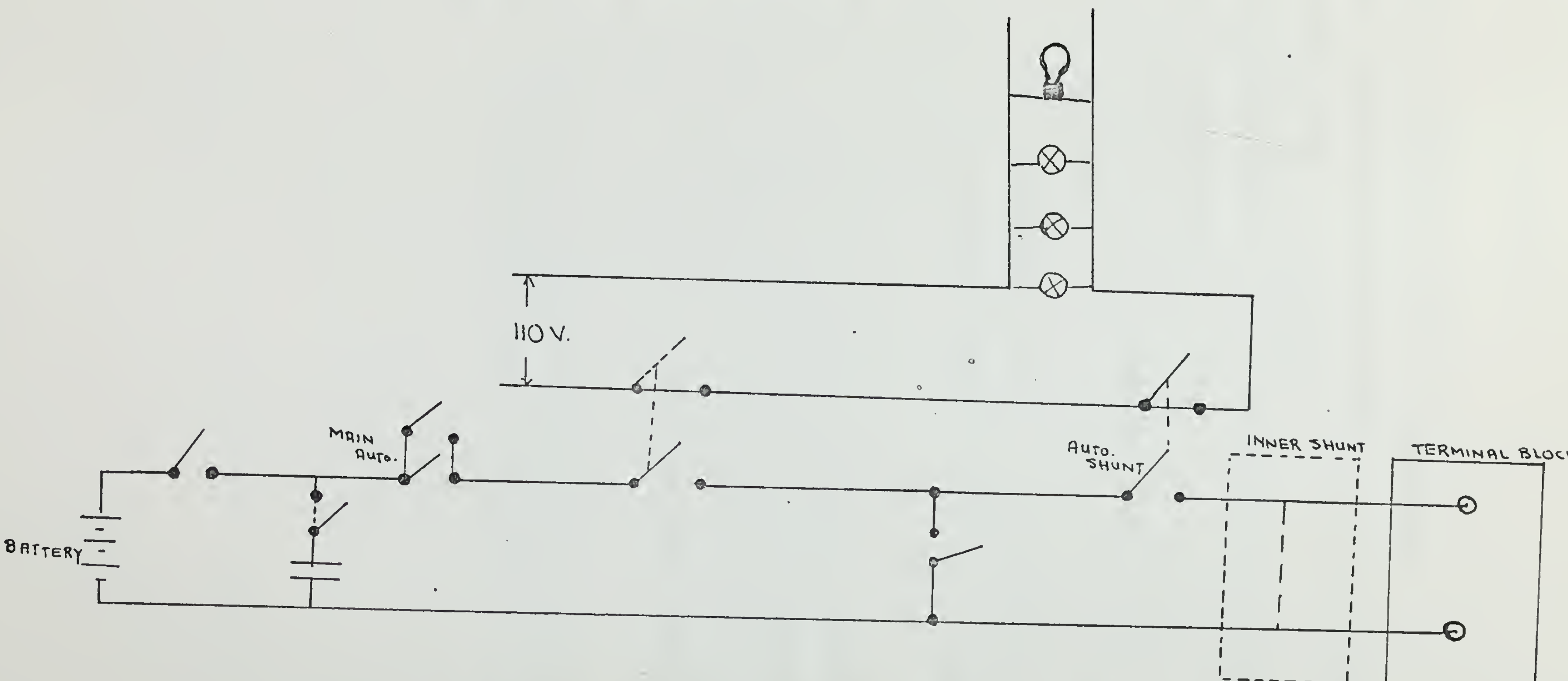

Firing and safety circuits of the chamber

APPENDIX G

THE NEGLECT OF TEMPERATURE RISE IN THE SPECIMENS

The following examples illustrate the effect of the temperature rise in the specimens due to the explosion.

Assume, a temperature change of 10°F in a specimen. This corresponds to 0.0001 strain for steel specimens, which in turn corresponds to 3.000 p.s.i. stress for the same material. If the temperature change in the specimen is 10°F and if the Young modulus is 30 x 10^6 p.s.i., $\eta_{SP.} = 10^{-5}$ and $\eta_{ST.} = 1/2 \times 10^{-5}$ then a strain gange mounted on the specimen would give an error of $\Delta T(\eta_{SP.} - \eta_{ST.}) \times E$ which is equal to 1500 p.s.i. Therefore, the error is quite significant.

Thermal stresses would be more important when they are combined with the loading stresses. Ref.(13) In elastic as well as in plastic range a sufficiently high temperature rise would effect the properties of the material such as Young modulus, yield point, strain hardening, stress-strain rate etc.

With these considerations in mind and assuming that the plates are to be subjected to a uniform heat source, the following mathematical model is presented.

Mathematical Model

Assumptions

1-) The plates are subjected to a uniform heat source, Q_o.

2-) The plates are attached to fixed boundaries.

3-) All of the physical properties of the plates are constant. i.e. are not functions of temperature.

4-) The rear surface of the plate, z = 0 and four edges are insulated.

5-) We have continuous heat source.

6-) Absorbed heat energy Q_o is equal to the explosive heat energy, Q.*

7-) Heat conduction in z direction only.

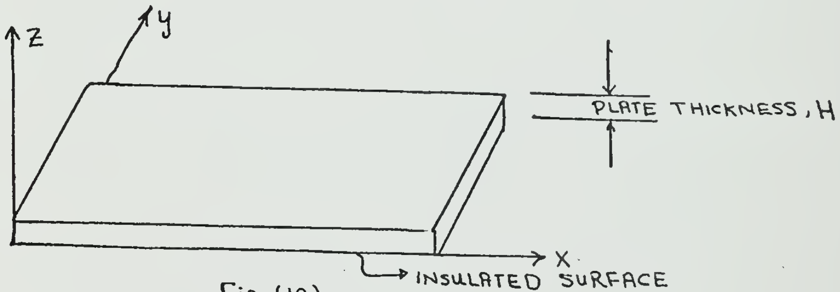

Fig. (18)

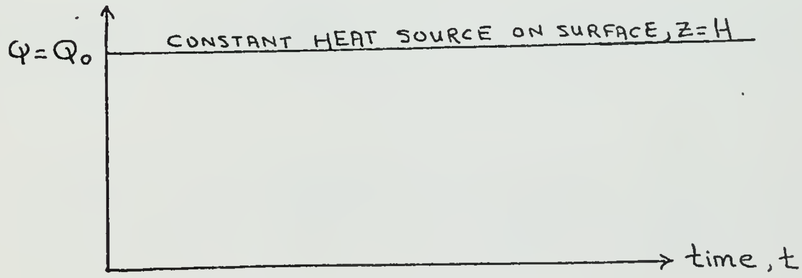

Fig. (19)

---

* Strictly speaking $Q \neq Q_o$. Since, some of the explosive heat energy is ratiated into the atmosphere.

The differential equation of the heat conduction relevant to a plate which is subjected to a sudden heat source is

$$\frac{\partial T(z,t)}{\partial t} = \alpha \frac{\partial^2 T(z,t)}{\partial z^2} \tag{5}$$

And the boundary conditions are:

$$k \frac{\partial T}{\partial z} = Q \quad \text{at} \quad z = H \quad \text{and} \quad t \geqslant 0^+$$

$$T = T_0 \quad \text{at} \quad t \leqslant 0^-$$

$$\frac{\partial T}{\partial z} = 0 \quad \text{at} \quad z = 0 \quad \text{and} \quad t \geqslant 0^+$$

Then, the solution of the equation (5) is given by Ref.(14).

$$T(z,t) = T_0 + \frac{QH}{k} \left\{ \frac{\alpha t}{H^2} + \frac{3z^2 - H^2}{6H^2} - \frac{2}{\pi^2} \sum_{n=1}^{\infty} \frac{(-1)^n}{n^2} e^{-\left(\frac{n\pi}{H}\right)^2 \alpha t} \cos \frac{n\pi z}{H} \right\}$$

or in the dimensionless form:

$$\frac{k(T - T_0)}{QH} = \frac{\alpha t}{H^2} + \frac{3z^2 - H^2}{6H^2} - \frac{2}{\pi^2} \sum_{n=1}^{\infty} \frac{(-1)^n}{n^2} e^{-\left(\frac{n\pi}{H}\right)^2 \alpha t} \cos\left(\frac{n\pi z}{H}\right) \Big\}$$

Since the infinite series in the last equation converges rapidly only the first term of the series will be retained for given values of z. The dimensionless temperature rise versus dimensionless time is shown in Fig.(20).

Fig.(20) enables us to calculate the temperature rise for a given values of time or vise versa.

As an example, suppose that a 0.173 in. thick steel plate is subjected to the explosive heat source induced by a detasheet explosive of 10 grams. Specimen surface area is 15.0 sq. in. Calculate the temperature rise on the Layer, Z = H/2 at the end of one microsecond. The following data is also available for the calculations.*

	STEEL (mild)	ALUMINUM (pure)
Thermal diffusion, :	0.452 ft^2/hr	3.665 ft^2/hr
Thermal conductivity, k :	25.0 Btu/hr-ft^{o}F	118.0 Btu/hr-ft-^{o}F
Density, ρ :	487.0 lbm/ft^3	169.0 lbm/ft^3
Specific heat, Cp :	0.113 Btu/lbm-^{o}F	0.214 Btu/lbm-^{o}F

Table (6)

Explosive heat = 1.100 cal/gram Ref.(16)

Conversion factor: 1 cal = 3.97×10^{-3} Btu.

---

* The values given in table (6) are adopted from Ref.(15).

Solution

Explosive heat energy, Q = 10 x 1100 x 3.97 x 10^{-3} = 43.67 Btu.

Assuming explosive heat source is uniform, as shown in Fig.(20) and using assumption - 6

$$\dot{Q}_o = \frac{43.67 \times 3600}{10^{-3} \times \frac{15}{144}} = 312 \times 10^6 \text{ BTU/hr-ft}^2$$

Dimensionless time, $\frac{\alpha t}{H^2} = \frac{0.452 \times 10^{-3}}{\left(\frac{0.173}{12}\right)^2 \times 3600} = 6.4 \times 10^{-4}$

From Fig.(20) corresponding temperature rise is: $\frac{\Delta T k}{\dot{Q}_o} \simeq 0$

Hence, $\Delta T = 0$

Conclusions of the Appendix

As long as the assumed uniform explosive heat energy takes one micro second or less, it is found that temperature rise and corresponding thermal stresses are negligible which, therefore, do not cause any errors in the readings of strain gages.

However, when the specimens are in direct contact with the explosive, another problem arises. High explosive temperature tends to create a pitted surface on the specimens.

Finally, even if the explosive pressures are below those necessary for spalling, then a rubbery type material which has good insulation characteristics could still be used to prevent pitting effect.

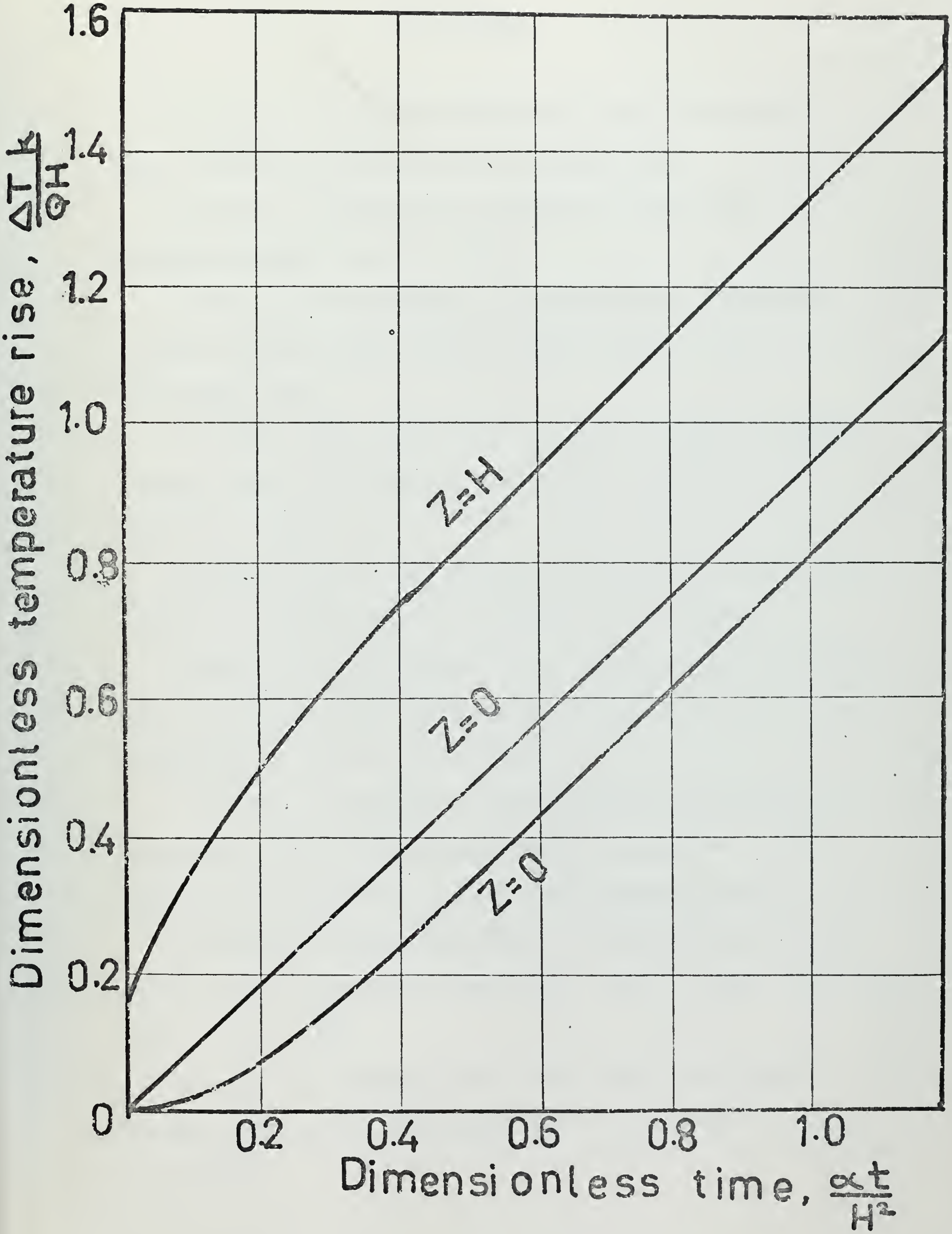

1.6
1.4
1.2
1.0
0.8
0.6
0.4
0.2
0
0.2
0.4
0.6
0.8
1.0
Z=H
Z=0
Z=0
Dimensionless temperature rise, $\frac{\Delta T k}{QH}$
Dimensionless time, $\frac{\alpha t}{H^2}$

Fig. 20

BIBLIOGRAPHY

1. JONES, N. "Finite Deflections of a Rigid Viscoplastic Strain hardening Annular plate loaded Impulsively"

2. JONES, N. "Unpublished class notes of 13.18 Ship Structural Dynamics", M.I.T., 1969.

3. LEE, E.H., and SYMONDS, P.S. "Large Plastic Deformation of beams under Transverse Impact". J. Appl. Mech. Vol.19, No.3, P.308, 1952.

4. HOPKINS, H.G., and PRAGER, W. "On the Dynamics of plastic Circular Plates". J. of Applied Mathematics and Physics Vol.5, P.22, No. 4, 1954.

5. FLORENCE, A.L., "Circular plate under a uniform Distributed Impulse". J. Applied Mechs. Vol. 32, No. 1, P. 7, 1965.

6. WANG, A.J., and HOPKINS, H.G., "On the plastic deformation Built-in Circular plates under impulsive load". J. Mech. and Physics of Solids, Vol. 3, No. 1, P. 22, 1954.

7. JONES, N. "Influence of strain hardening and strain rate sensitivity on the permanent deformation of impulsively loaded rigid-plastic beams". Int. J. Mech. Sci. Pergamon Press Ltd.

8. JONES, N. "Finite Deflections of a Simply Supported Rigid-plastic Annular Plate Loaded Dynamically". Int. J. Solids Structures Vol. 4, P. 593, 1968.

9. JONES, N. "Combined Distributed loads on Rigid-plastic Circular plates with large deflections". Int. J. Solids, Vol. 5, P. 51, 1969.

10. COX, A.D., and MORLAND, L.W., "Dynamic plastic Deformations of simply supported square plates". J. Mech. and Physics of Solids, Vol. 7, P. 229, 1959.

11. GERARD, G. and PAPIRNO, R., "The impact tube technique for Dynamic stress-strain measurements". IX Congrès Int. de Mecanique Appliquée, Tome VIII, p.439, 1957.

12. GOLDSMITH, W., "Impact". Edward Arnold (publishers) Ltd. 1960.

13. GATEWOOD, B.E., "Thermal Stresses", Mc. Graw-Hill Book Company, Inc. 1957.

14. CARSLAW and JAGER J.C., "Conduction of Heat in Solids". Oxford University Press, second edition, 1959.

15. ROHSENOW W.M. and CHOI H., "Heat, Mass, and Momentum Transfer". Prentice-Hall, Inc. 1961.

16. AMERICAN ORDNANCE ASSOCIATION, NAVAL WEAPONS STATION, "Detasheet Loading Application" June 22, 1967.

17. BRANDRUP, J. and IMMERGUT E.H. (Editors), "Polymer Handbook", P. VI-65, Interscience Publishers, New York, 1966.

18. BAER, E. (Editor), "Engineering Design for Plastics", P.1003, Reinhold Publishing Corporation, London, 1964.

19. LYMAN, T. (Editor), "Metals Handbood",1948 edition, The American Society for Metals, 1948.

NOMENCLATURE

Symbols

A	:	Impact velocity computed using Equation 4
Cp	:	Specific heat
D	:	Distance from ground to bottom of ballistic pendulum
E	:	Young modulus
ϵ	:	Strain
g	:	Gravition force, 32.1724 ft./sec^2
H	:	Specimen thickness
I	:	Moment of inertia of the ballistic pendulum
i	:	Moment of inertia of the specimen
K	:	Thermal conductivity
L	:	Short length of the specimen, L = 3.0 in.
m	:	Specimen weight
M	:	Pendulum weight
(m+M)	:	Total pendulum weight (includes ballast and specimen weights)
μ	:	Density times plate thickness, $\mu = \rho \times H$
$\eta_{sp.}$	:	Thermal expansion coefficient of a specimen
$\eta_{st.}$	:	Thermal expansion coefficient of a strain gage.
Q	:	Explosition heat energy
Qo	:	Absorbed heat energy
R	:	Distance from pivot to center of gravity of a specimen
R_1	:	Distance form pivot to heat sensitive paper
R*	:	Distance form pivot to center of gravity of the pendulum
R-R*	:	Shifting of center of gravity due to ballast loads
ρ	:	Density

Symbols

S	:	Specimen surface area
Sp.No	:	Specimen number
σ	:	Stress
σ_o	:	Yield stress
T	:	Temperature
To		Room temperature
ΔT	:	Temperature rise, (T-To)
t	:	Time
ΔT	:	T-To = temperature rise in a specimen
Vo	:	Impact velocity
Vel	:	Impact velocity calculated using Equation 3
W	:	Final deformation
Wm $\equiv$	:Wmax:	Max. final deformation
ω_o	:	Angular initial velocity of the ballistic pendulum
γ	:	Hingle line angle on a rectangular plate
θ_m	:	Maximum forward swing angle of the ballistic pendulum
$+\delta$	:	Maximum forward amplitude
$\frac{\alpha t}{H^2}$	:	Dimensionless time
$\frac{\Delta T k}{Q_o}$	:	Dimensionless temperature rise
α	:	Thermal diffusivity